

Responses to Referee #1:

This research article investigates the impact of anthropogenic aerosol reductions in China on Australia's climate. The study found that the decline in China's aerosols since 2013 contributed to drier and warmer conditions in Australia by altering temperature and pressure gradients, which intensified the Southern Trade Winds and caused moisture divergence over Australia. The study also links these climate changes to an increase in wildfire risks in Australia. This research highlights the significant influence of distant aerosols on regional climate and offers insights for drought and wildfire risk mitigation.

The manuscript is interesting, well written and tackles an important topic of research (i.e., impact of Chinese aerosols on Australian climate). However, some technical details between the comparison of modelling results and observations need to be corrected and the selection of figures should be adjusted. I recommend acceptance of the manuscript if the major comment below can be addressed.

We thank the reviewer for the constructive suggestions, which are very helpful for improving the clarity and reliability of the manuscript. Please see our point-by-point responses (in blue) to your comments below.

Major comments

One of my main comments is related to the comparison of observation/reanalysis data and simulated results: There seems to be some inconsistency between the timeperiods used. In the method section it is mentioned that the period 2013-2019 is used for the observation/reanalysis data as well as the simulated data. However, in the captions of the supplementary figures as well as in the description of these figures in the text (e.g. L274, 278) it is mentioned that the observations are for 2010-2019. Please clarify if the same timeperiod is used for observation/reanalysis data and modelling data and if that is not the case, the plots have to be redone for the correct timeperiod to ensure an accurate comparison. Besides, is this warming and drying trend over Australia still continuing or why did the authors look at the time period 2013-2019?

The warming and drying trends in Australia due to the reduction of aerosols in China were simulated based on the two simulations with anthropogenic emissions of aerosols and precursors at years 2013 and 2019. It is because China implemented the "Air Pollution Prevention and Control Plan" in 2013 and established nationwide PM_{2.5} observation sites in 2013. Whether the simulated climate responses can be detected in the real world requires the observational evidence. However, the seven years of period 2013–2019 are too short to fully capture the trends in climate variables, as various natural variabilities could influence temperature and rainfall in Australia. For example, climate variabilities, such as ENSO, can have significant impacts on the Australian monsoon and rainfall patterns and influence the long-term trends of temperature and precipitation in Australia. Therefore, we included more years to calculate the trends of the climate variables in observations. It will not affect the results since that the aerosol reductions in China only account a small amount of the changing climate in Australia. We have now added the explanation in the manuscript as "Note that, the trends in observations are calculated during 2010–2019 to minimize the internal

variability.”. Regarding whether the trend is continuing, CSIRO and BOM (2022) reported that the warming is still ongoing in Australia and the drying trend is still ongoing in Northern Australia, which could be contributed by the further reductions in Asian aerosols.

While it is great that the author’s tried to reduce the figures in the main text to only 4 to explain the whole story, in particular the mechanistic analysis (Section 3.2) is difficult to follow for the reader with the limited number of figures. For instance, a combination of Figure S16 and S17 (i.e. the filled contours showing the SST pattern overlaid by the climatological wind field) would be a relevant figure to show. Additionally, Figure S21 is heavily referenced in the manuscript but the figure is only shown in the supplementary. Besides, maybe a small schematic of the described mechanism similarly as in Fahrenbach et al. 2024 would be helpful to guide the reader through the description.

As requested, we have moved several figures in the main text and added the schematic diagram as shown below.

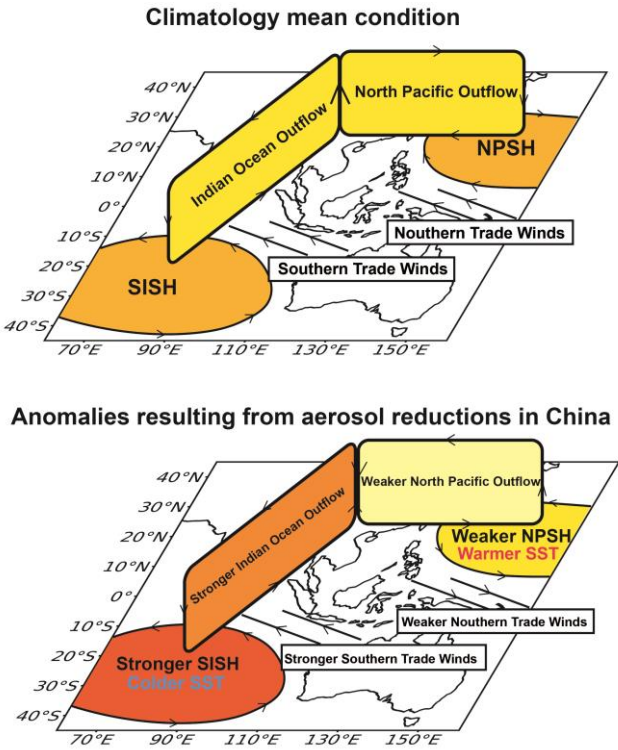


Figure 6. Schematic of the response in large-scale 3D circulations in the Asian-Pacific region to aerosol reductions in China. The top panel shows climatology mean condition, and the bottom panel shows anomalies resulting from aerosol reductions in China.

On the topic of figures, it would be important to show a comparison of the simulated changes with the observed precipitation pattern (Figure S8) as well as the observed wind changes (Figure S18). This is particularly relevant since the authors are trying to do an “attribution” study and it has to be quantified that the observed and modelled changes agree. Additionally, the authors claim that the modelled and observed wind changes are similar (L319-321). While I do acknowledge that 3D wind changes are not the most reliable fields in reanalysis data, this is a bit of an overstatement.

Figure S18b and c show very few significant changes making it difficult to understand the simulated flow and Figure S18d shows the largest significant trends in the winds east of Borneo and around stronger southern Trade winds based on the simulated data. Maybe the authors could think about showing all wind vectors and colouring the significant ones in, so that the reader can at least see if the observations show the same trend even if they might not be significant based on this test?

Thank you for your suggestion. We have revised the figure displaying the 3D wind fields, with significant and insignificant circulations clearly distinguished. Additionally, the statement has been revised to: “Although only a few significant changes persist in Northern Australia, the large-scale circulations around Australia show noticeable similarities to the simulated results.” to avoid the overstatement.

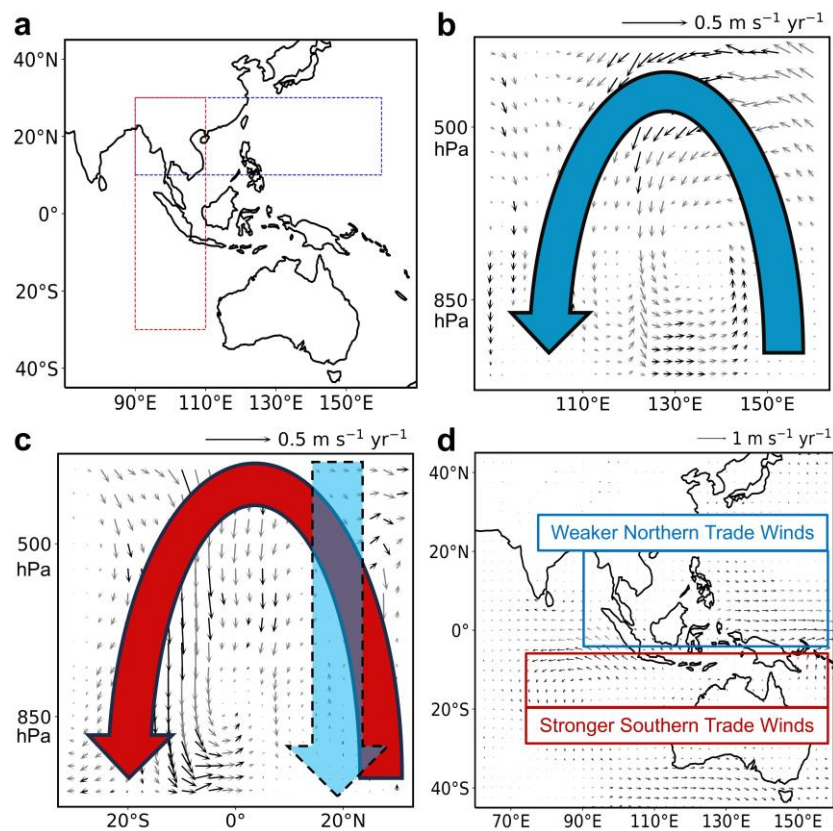


Figure S17. Linear trends in observed vertical circulations and 850 hPa wind fields in Asia-Pacific regions. Panel b and c shows pressure–longitude and latitude cross-section of linear trends in annual mean atmospheric circulations (unit: m s^{-1} , vectors) over areas marked with the blue and red box in panel a during 2010–2019 from ERA5. Panel d shows linear trends of wind fields (unit: m s^{-1} , vectors) at 850 hPa in Asia-Pacific regions. Trends of atmospheric circulations and winds which are statistically significant at the 90% confidence level are shown in black, while the insignificant ones are shown in grey.

My last comment regarding the figures is that the figure S15 should also be included in the main

text. It seems biased to try to find a link / attribution but only show the plots for China which the authors have identified as the relevant one. Maybe a figure showing the annual precipitation trends for CHN, OTH, NA+EU and then a seasonal plot for the CHN plots would be best?

As requested, we have moved the figure in the main text and showed the CHN, OTH, NA+EU (Figure 1 below) and then a seasonal plot for the CHN (Figure 2 below).

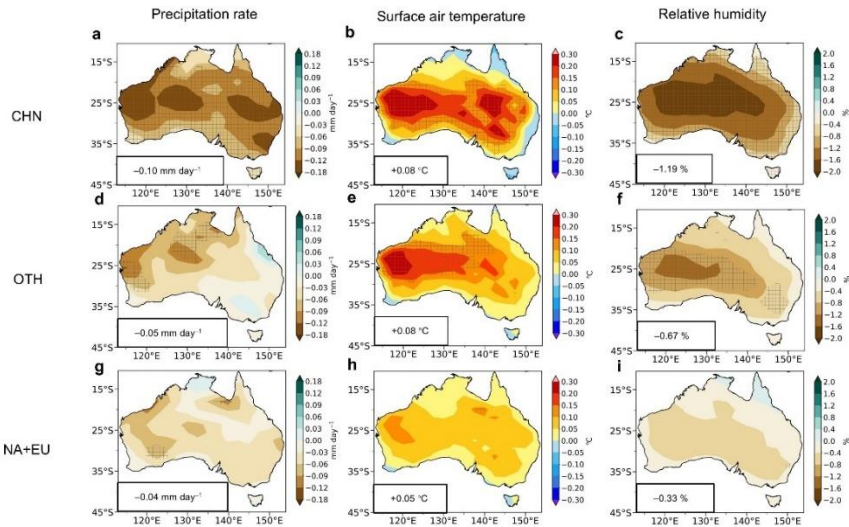


Figure 1. Simulated changes in precipitation rate, surface air temperature and relative humidity in Australia due to aerosol changes between 2013 and 2019. Spatial distributions of simulated differences in annual mean precipitation rate (Pr, **a**, **d**, and **g**, unit: mm day^{-1}), surface air temperature (TS, **b**, **e**, and **h**, unit: $^{\circ}\text{C}$) and relative humidity (RH, **c**, **f**, and **i**, unit: %) in Australia between BASE and CHN (CHN minus BASE, **a–c**), between BASE and OTH (OTH minus BASE, **d–f**), and between BASE and NAEU (NAEU minus BASE, **g–i**). The shaded areas indicate results are statistically significant at the 90% confidence level. Regional averages over Australia are noted at the bottom-left corner of each panel.

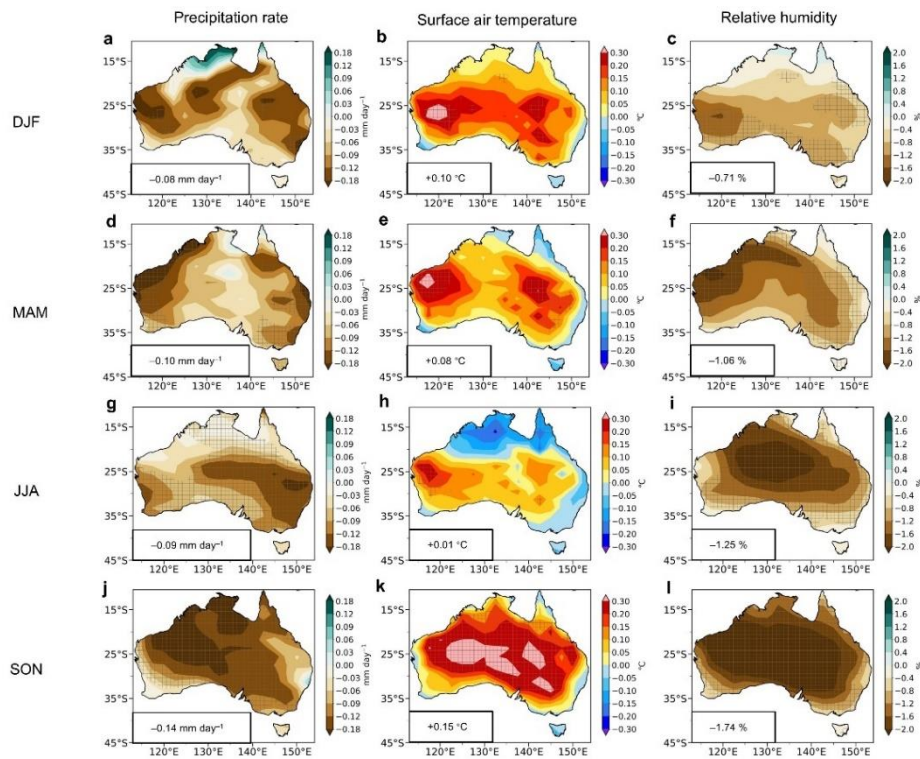


Figure 2. Simulated changes in precipitation rate, surface air temperature and relative humidity in Australia due to aerosol changes in China between 2013 and 2019. Spatial distributions of simulated differences in DJF (December, January and February, a–c), MAM (March, April and May, d–f), JJA (June, July and August, g–i) and SON (September, October and November, j–l) mean precipitation rate (Pr, a, d, g, and j, unit: mm day⁻¹), surface air temperature (TS, b, e, h, and k, unit: °C) and relative humidity (RH, c, f, i, and l, unit: %) in Australia between BASE and CHN (CHN minus BASE). The shaded areas indicate results are statistically significant at the 90% confidence level. Regional averages over Australia are noted at the bottom-left corner of each panel.

The authors discuss the influence of the (very strong) low bias in PM_{2.5} in CESM1 compared to the observations in L385-388, which is good and relevant. However, this should also be mentioned throughout the manuscript, for instance when the authors try to estimate very precise values for the influence of the Chinese aerosol reductions on precipitation and temperature (L270-271).

To address this, we have now included notes regarding this low bias and its potential impact on the accuracy of these estimates in the relevant sections throughout the manuscript, such as: “However, considering that aerosols are underestimated in the model, the impact of aerosol reductions in China on Australia’s climate/wildfire risks may also be underestimated.”

Minor comments

L29-31: The times mentioned in this sentence seem confusing since when first reading it seems that a trend from 2013 is caused by something happening around the 2010s. Maybe using

119 “conditions since the 2010s” would help to settle this confusing sentence.

120 Revised.

121 L68-70: Please change “increasing GHGs” to increasing GHG emissions.

122 Changed.

123 L72-75: This sentence is very long and confusing, please split it up into two or shorten it

124 This sentence has been shortened as: “Atmospheric aerosols are the second-largest anthropogenic
 125 climate forcer, exerting an overall cooling effect that partially masks the warming induced by
 126 GHGs.”

127 L73: “Earth’s” instead of “earth’s”

128 OK.

129 L104: “especially in northern Australia/especially in the North of Australia” instead of “especially
 130 the northern Australia”

131 Revised.

132 L104: “affected by the Australian monsoon” instead of “affected by Australian monsoon”

133 Revised.

134 L153-159: Is there a reason for the choice of the GPM dataset rather than for instance GPCP data?

135 “GPM provides higher temporal and spatial resolution data compared to GPCP, making it more
 136 suitable for studies focused on short-term precipitation variability and regional climate dynamics.”
 137 The statement has been added to the manuscript.

138 L224: “Earth’s surface” instead of “earth’s surface”

139 Revised.

140 L244: The setting of DF to 10 according to Sharples et al 2009 needs some more explanation. At
 141 least one sentence why Sharples et al choose this value and why it is also applicable here.

142 Thank you for your suggestion. Sharples et al. (2009) mentioned that “Such a factor will have no
 143 real bearing on the methods of comparison employed in the later sections of the paper and so for
 144 convenience we assume that $DF = 10$ in what follows.” We acknowledge that this assumption is
 145 idealized. To address this, we have calculated gridded DFs (Figure S7 below) and found that the
 146 DFs in Australia are close to 10, with spatial distributions being nearly homogeneous. Therefore,
 147 setting $DF = 10$ for Australia is reasonable in this context.

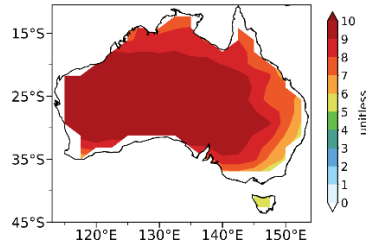


Figure S7. Spatial distributions of annual mean dry factor (unit: unitless) in Australia during 2010–2019. The data is from fire danger indices historical data from the Copernicus Emergency Management Service (CEMS, 2019; Vitolo et al., 2020).

Additionally, we compare FFDI with $DF = 10$ and FFDI with the gridded DF (Figure S8 below). The patterns and regional averages of both are similar.

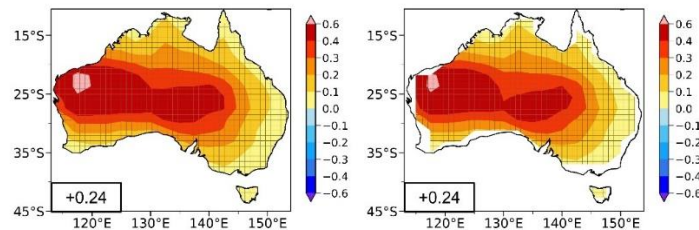


Figure S8. Spatial distribution of simulated changes in FFDI (unit: unitless) during fire seasons in Australia between BASE and CHN (CHN minus BASE). Shaded areas indicate results that are statistically significant at the 90% confidence level. Regional averages for Australia are noted at the bottom-left corner of each panel. The left panel shows FFDI ($DF = 10$), and the right panel shows FFDI (gridded DF).

L277: Please change “evidence“ to “indication“.

Changed.

L389: Please use “Earth System Model” or “fully-coupled climate model” instead of “aerosol-climate model” which would imply to me that this model is not fully coupled (which is the case according to the method section)

Thanks for your reminder. The term “aerosol-climate model” has been replaced with “fully-coupled climate model” throughout the manuscript, as suggested.

Figure S3: The colourbar of these two plots should be the same as the reader might be tricked into thinking that the magnitude changes between the observed and modelled data are similar.

Thank you for your suggestion. If we use the same color scale for both plots, the color range of the modeled results becomes overly uniform. However, we have now added a note in the figure caption to remind the reader that the magnitudes of the observed and modeled data are not directly comparable, and that the color scales represent different ranges.

173

174 **References:**

175 CSIRO and BOM: State of the Climate 2022, 2022

176 CEMS: Fire danger indices historical data from the Copernicus Emergency Management
177 Service, <https://doi.org/10.24381/cds.0e89c522>, 2019.

178 Vitolo, C., Di Giuseppe, F., Barnard, C., Coughlan, R., San-Miguel-Ayanz, J., Libertá, G., and
179 Krzeminski, B.: ERA5-based global meteorological wildfire danger maps, Sci. Data, 7, 216,
180 <https://doi.org/10.1038/s41597-020-0554-z>, 2020.

181

Responses to Referee #2:

The manuscript investigates the role of the recent decline in East Asian anthropogenic aerosols in driving precipitation and temperature changes across Australia. The authors highlight the potential for aerosols to contribute to enhancing the fire risk via widespread drying and warming. The topic is timely and very important, as not many studies have examined the influence of recent changes in aerosols on recent climate variations. However, I find several major weaknesses in the study, including in the simulation design, that prevent the manuscript from being acceptable for ACPD. Unfortunately, I need to recommend a rejection. Happy though to reconsider the manuscript if reviewed accordingly.

Thank you for your feedback. We will carefully consider the points you raised regarding the simulation design and other aspects of the study. We value your insights and will make every effort to improve the quality of our work. We would be grateful for your reconsideration of the manuscript. Please see our point-by-point responses (in blue) to your comments below.

Major comments:

I believe there is a serious overinflation of the recent observed rainfall changes over Australia. Firstly, the authors use observations and plot linear trends from 2010, while model results are shown as 3-year differences from 2013. While the latter accounts for the decline in aerosols, observations show that the years 2010 and 2011 were anomalously wet over Australia, and just a couple of years before rainfall was much less (I have checked by plotting observations since 2000). This can also be inferred by examining Fig 2, where clearly the trend in panel d is affected by the two early years. By eye, using 3-year composites from 2013, the rainfall changes are very modest. Looking at more recent years, it turns out that 2019 was also anomalously dry, and more recent years (excluding those affected by COVID-related reduced emissions) show a recovery. Therefore the results based on observations, which ultimately is the motivation of the study, are strongly affected by the extremely short record and cannot be trusted.

Thank you for pointing out the strong variability in rainfall in Australia. We agree with reviewer that the observed trend of rainfall could be affected by the wet years in 2010/2011 and dry year in 2019, which could be induced by the interval variability (such as ENSO). However, we could not deny the decreasing precipitation during 2010–2019 and rule out the potential influence of changing aerosols on the rainfall variation. Additionally, we are trying to quantify the role of aerosol reduction in China in the Australian climate, rather than fully attribute to changing Australian climate to aerosols in China, considering that aerosol reductions in China are found to contribute to small part of the changing precipitation in Australia. The simulation results are still robust enough to support our conclusions because our model experiments are based on validated climate model, providing strong evidence that aerosol reductions in China have a significant impact on Australia's climate.

In fact, the emission reduction of aerosols and precursors in China starts in 2010 rather than 2013. We chose the year 2013 in simulation was because China implemented the “Air Pollution Prevention and Control Plan” in 2013 and established nationwide PM_{2.5} observation sites in 2013. As the reviewer mentioned, Australia experienced a transient from dry years before 2010 to wet years in 2010/2011 and the rainfall recovery after 2020. It is also in accordance with the increasing

aerosols in China before 2010 and the slowdown in aerosol reduction in recent years. But it still requires quantitative analysis.

Related to the point above, it is not surprising that observed circulation trends (e.g., Fig. S18) are extremely weak. Yet, this is the mechanism driving Australian rainfall changes, thus is central to the proposed aerosol influence.

As mentioned earlier, given natural variability and the multiple factors influencing precipitation in Australia, it is quite challenging to capture patterns in the observations that resemble the results of the sensitivity experiment on China's aerosol reductions. We have redrawn the circulation figure (Figure S17 below), displaying all circulations regardless of whether they pass the significance test. Notably, we can observe clear similarities with the model results.

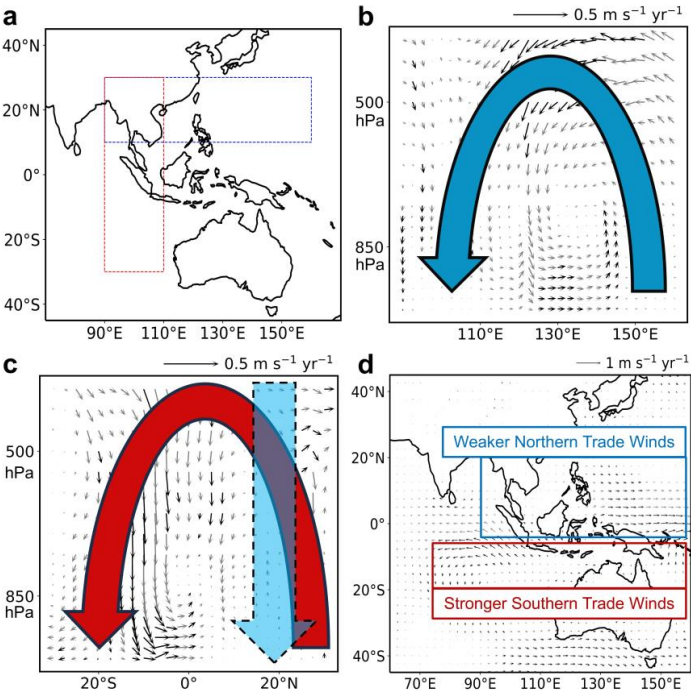


Figure S17. Linear trends in observed vertical circulations and 850 hPa wind fields in Asia-Pacific regions. Panel b and c shows pressure–longitude and latitude cross-section of linear trends in annual mean atmospheric circulations (unit: m s^{-1} , vectors) over areas marked with the blue and red box in panel a during 2010–2019 from ERA5. Panel d shows linear trends of wind fields (unit: m s^{-1} , vectors) at 850 hPa in Asia-Pacific regions. Trends of atmospheric circulations and winds which are statistically significant at the 90% confidence level are shown in black, while the insignificant ones are shown in grey.

The model analysis is also weak in the sense that 3-year composites are extremely short to identify forced trends. In addition, observed trends should be first compared to those from a control simulation and the contribution of aerosols should be related to the model world, not observations.

We believe there may be a misunderstanding regarding the 3-year composites mentioned by the

reviewer. In our study, we did not use 3-year composites for climate variables (only for PM_{2.5} and AOD in observations since they are more linear than climate variables). Our equilibrium experiment designs have been described in the 2.2 Model Description and Experimental Design section.

Regarding the model comparison, we would like to clarify that due to the nature of our equilibrium experiments, direct comparison with baseline control experiments is not feasible. Even in transient simulations, models may not be able to fully capture the short-term and complex observational signal, as observational data are influenced by numerous factors over short time periods. However, models can provide a quantitative evaluation of how specific factors, such as aerosols, might contribute to climate phenomenon. This approach has been commonly used in previous studies (Bollasina et al., 2011; Heede and Fedorov, 2021; Hwang et al., 2024; Vecchi et al., 2006; Wang et al., 2023; Yang et al., 2022) to isolate the impact of individual forcings. This limitation has been noted in the discussion section: “Another limitation of this study is that we calculated the relative contribution of aerosol changes in China to the changing climate in Australia by combining model simulations and observational data, which could lead to the inconsistency and introduce biases to the quantitative results.”.

Another major weakness is the experimental design. The authors examine long-term changes coming from equilibrium runs, which are far from representing the actual transient response over 10 years or so. This is likely far from being in equilibrium. I would have seen large-ensemble transient simulations with time-varying aerosols (2013-2024 for example) as more appropriate and suitable.

We appreciate the reviewer’s concern regarding the use of equilibrium runs and the suggestion to use large-ensemble transient simulations. While transient simulations offer a more dynamic representation of temporal changes, the relatively short period from 2013 to the present may not provide enough time for the climate system to fully respond to aerosol changes. This is particularly true when considering the long timescales required for oceanic heat capacity to equilibrium. Furthermore, equilibrium simulations allow for a clearer isolation of the forced response to aerosol changes, minimizing the impact of short-term climate variability.

We do acknowledge, however, that transient simulations would offer a more accurate depiction of the time-varying effects of aerosol reductions, especially as aerosol reductions in China continue. As the climate system responds more robustly over time, transient simulations will likely become a more appropriate tool. Therefore, while equilibrium simulations are potentially more suitable for the present study, we plan to use transient simulations in future research.

We have also mentioned the limitation of not using transient simulations in the discussion section: “While this study relies on equilibrium simulations to isolate the forced response to aerosol changes, we acknowledge that transient simulations, which account for time-varying aerosol reductions, would provide a more accurate depiction of the dynamic climate system response. Given that aerosol reductions in China continue to evolve, transient simulations would be more appropriate for capturing the full temporal effects of these changes. Large-ensemble transient simulations are suggested in future studies to better represent the evolving aerosol-climate interactions over time and to enhance the robustness of the findings.”.

Trends or changes should always be plotted with the related statistical significance, such as in Figs. 1 and 2.

Thank you for the suggestion. Now all trends or changes have been plotted with statistical significance.

Fig 3: I think it would be more appropriate to display the divergent wind, rather than the total wind.

We chose to display the total wind in Figure 3 to highlight the strengthening of Southern Trade Winds. For the divergent winds, we also displayed moisture divergence (Figure S18), which is more directly related to the changes in precipitation patterns that we are investigating.

References:

- Bollasina, M. A., Ming, Y., and Ramaswamy, V.: Anthropogenic Aerosols and the Weakening of the South Asian Summer Monsoon, *Science*, 334, 502–505, <https://doi.org/10.1126/science.1204994>, 2011.
- Heede, U. K. and Fedorov, A. V.: Eastern equatorial Pacific warming delayed by aerosols and thermostat response to CO₂ increase, *Nat. Clim. Chang.*, 11, 696–703, <https://doi.org/10.1038/s41558-021-01101-x>, 2021.
- Hwang, Y.-T., Xie, S.-P., Chen, P.-J., Tseng, H.-Y., and Deser, C.: Contribution of anthropogenic aerosols to persistent La Niña-like conditions in the early 21st century, *Proc. Natl. Acad. Sci. U. S. A.*, 121, e2315124121, <https://doi.org/10.1073/pnas.2315124121>, 2024.
- Vecchi, G. A., Soden, B. J., Wittenberg, A. T., Held, I. M., Leetmaa, A., and Harrison, M. J.: Weakening of tropical Pacific atmospheric circulation due to anthropogenic forcing, *Nature*, 441, 73–76, <https://doi.org/10.1038/nature04744>, 2006.
- Wang, P., Yang, Y., Xue, D., Ren, L., Tang, J., Leung, L. R., and Liao, H.: Aerosols overtake greenhouse gases causing a warmer climate and more weather extremes toward carbon neutrality, *Nat. Commun.*, 14, 7257, <https://doi.org/10.1038/s41467-023-42891-2>, 2023.
- Yang, Y., Ren, L., Wu, M., Wang, H., Song, F., Leung, L. R., Hao, X., Li, J., Chen, L., Li, H., Zeng, L., Zhou, Y., Wang, P., Liao, H., Wang, J., and Zhou, Z.-Q.: Abrupt emissions reductions during COVID-19 contributed to record summer rainfall in China, *Nat. Commun.*, 13, 959, <https://doi.org/10.1038/s41467-022-28537-9>, 2022.

Dry and warm conditions in Australia exacerbated by aerosol reduction in China

Jiyuan Gao¹, Yang Yang^{1*}, Hailong Wang², Pinya Wang¹, Hong Liao¹

¹Joint International Research Laboratory of Climate and Environment Change (ILCEC), Jiangsu
Key Laboratory of Atmospheric Environment Monitoring and Pollution Control, Jiangsu
Collaborative Innovation Center of Atmospheric Environment and Equipment Technology,
School of Environmental Science and Engineering, Nanjing University of Information Science
and Technology, Nanjing, Jiangsu, China

²Atmospheric, Climate, and Earth Sciences Division, Pacific Northwest National Laboratory,
Richland, Washington, USA

*Correspondence to yang.yang@nuist.edu.cn

Abstract

A substantial decline in anthropogenic aerosols in China has been observed since the initiation of clean air actions in 2013. Concurrently, Australia experienced anomalously dry and warm conditions ~~in~~since the 2010s. This study reveals a linkage between aerosol reductions in China and the drying and warming trends in Australia during 2013–2019 based on ~~aerosol~~-fully-coupled climate model simulations and multi-source observations. Aerosol decline in China triggered alterations in temperature and pressure gradients between the two hemispheres, leading to intensified outflow from Asia towards the South Indian Ocean, strengthening the Southern Indian Subtropical High and its related Southern Trade Winds. Consequently, this atmospheric pattern resulted in a moisture divergence over Australia. The reduction in surface moisture further resulted in more surface energy being converted into sensible heat instead of evaporating as latent heat, warming the near-surface air. Aerosol reductions in China are found to contribute to 19% of the observed decreases in precipitation and relative humidity and 8% of the increase in surface air temperature in Australia during 2013–2019. The intensified dry and warm climate conditions during 2013–2019 further explain 12%–19% of the increase in wildfire risks during fire seasons in Australia. Our study illuminates the impact of distant aerosols on precipitation and temperature variations in Australia, offering valuable insights for drought and wildfire risk mitigation in Australia.

1 Introduction

Australia encompasses various climate zones, ranging from the tropical climate in the north to arid conditions in the interior and temperate climates in the south (Head et al., 2014). The continent is predominantly dry, receiving an average annual rainfall of less than 600 mm and less than 300 mm over half of the land. Evident long-term trends can be observed in Australia's historical rainfall records. These trends reveal a notable shift towards drier conditions across southern Australia (Dey et al., 2019a; Nicholls, 2006; Rauniyar and Power, 2020; Wasko et al., 2021), and an increase in rainfall before 2010 (Dey et al., 2019a, b; Evans et al., 2014; Nicholls, 2006; Rotstayn et al., 2007; Wasko et al., 2021) followed by a slight decreasing trend of rainfall after 2010 (CSIRO and BOM, 2022) in the northern Australia.

Precipitation in Australia is influenced by a variety of atmospheric circulation systems, including East Coast Lows (ECLs), the Australian-Indonesian Monsoon, tropical cyclones (TCs), fronts, and different modes of large-scale climate variabilities, such as the El Niño-Southern Oscillation (ENSO), Indian Ocean Dipole (IOD), Interdecadal Pacific Oscillation (IPO), Subtropical ridge (STR), Southern Annular Mode (SAM), and Madden Julian Oscillation (MJO) (Dey et al., 2019a; Risbey et al., 2009). The linkages between Australia's rainfall characteristics and these drivers could change in response to the internal natural variabilities and external anthropogenic forcings. Rauniyar and Power (2020) reported that the drier conditions across the southern Australia could be attributed to a combination of both decadal-scale natural variability and changes in large-scale atmospheric circulation patterns, which was linked to the escalating emissions of greenhouse gases (GHGs), while Rotstayn et al. (2007) found that the increased levels of rainfall in northern Australia before 2010 was linked to the increases in aerosols in Asia.

Human activities have led to a rise of global surface air temperature by approximately 1.29 °C (0.99 to 1.65 °C) from 1750 to 2019, mainly due to an enhanced greenhouse effect from increasing ~~GHGs~~GHG emissions (IPCC, 2021). In addition to GHGs, human activities also emit a variety of aerosols and their gaseous precursors into the atmosphere. Since industrialization, there has been a significant rise in the levels of aerosols and precursors (Hoesly et al., 2018). ~~These atmospheric~~Atmospheric aerosols ~~play a crucial role in changing the earth's radiation balance, both directly and indirectly, and are considered as~~are the second-largest anthropogenic climate

forcer ~~following GHGs~~, exerting an overall cooling effect that partially masks the warming induced by GHGs (IPCC, 2013, 2021). However, as anthropogenic aerosols declined during the past decades in many countries of the world related to the clean air actions, the associated “unmask” effect is likely to exacerbate GHG-induced warming (Kloster et al., 2010). For example, in the 1980s, clean air actions were implemented in North America and Europe, leading to a decrease in the emissions of aerosols and their precursors (Hoesly et al., 2018). Reductions in aerosol emissions in the U.S. have led to changes in aerosol direct radiative forcing (DRF) by 0.8 W m^{-2} and indirect radiative forcing (IRF) by 1.0 W m^{-2} over the eastern U.S. during 1980–2010 (Leibensperger et al., 2012). Similarly, aerosol decreases over Europe between the 1980s and 1990s have caused a change in regional DRF by 1.26 W m^{-2} (Pozzoli et al., 2011). In China, the emissions of aerosols and their precursors have been reduced since 2013 due to the implementation of Air Pollution Prevention and Control Action Plan. Dang and Liao (2019) reported a 1.18 W m^{-2} change in DRF between 2012 and 2017 due to decreased aerosol levels over eastern China. Gao et al. (2022) estimated a warming of $0.20 \text{ }^{\circ}\text{C}$ in China, $0.15 \text{ }^{\circ}\text{C}$ in North America, and $0.14 \text{ }^{\circ}\text{C}$ in Europe, attributed to the decreases in aerosols during 2013–2019.

Monsoonal rainfall serves as a vital resource for agriculture, industry, and ecosystems across the monsoon-affected regions, affecting approximately two-thirds of the world’s population (B. Wang et al., 2021). Apart from GHGs-induced warming (Cook and Seager, 2013) and nature variabilities (e.g., ENSO) (Oh and Ha, 2015), aerosol also modulates monsoon system mainly through changing land-sea temperature and pressure gradient. The impact of aerosols on Asian monsoon has been widely investigated. Based on climate model simulations, Liu et al. (2023) found that aerosol reductions in East Asia during 2013–2017 resulted in an approximately 5% increase in the strength of the East Asian summer monsoon (EASM). The EASM is also reported to enhance due to future aerosol reductions from 2000 to 2100 (Wang et al., 2016). Dong et al. (2019) explored the effects of increased aerosol in Asia from 1970s to 2000s on atmospheric circulation and rainfall patterns and found anomalous moisture convergence and increased precipitation over the Maritime continent. Non-Asian aerosols also have an effect on South Asian monsoon rainfall through changes in the interhemispheric temperature gradient and meridional shifts of the Intertropical Convergence Zone (Bollasina et al., 2011, 2014; Cowan and Cai, 2011; Undorf et al., 2018). Australia, especially ~~thein~~ northern Australia, is largely affected by the Australian monsoon, which is characterized by winds that blow from the southeast during cold

season and from the northwest during the warm season (Gallego et al., 2017; Heidemann et al., 2023). Australia has a relatively low level of anthropogenic aerosols, which suggests that the impact of domestic anthropogenic aerosols on Australian monsoon should not be significant. However, the impact of remote aerosols on Australian monsoon have been investigated in previous studies, and they reported that the increases in Asian aerosols could enhance rainfall in Australia through increasing monsoonal winds towards Australia (Rotstayn et al., 2007; Fahrenbach et al., 2023).

Wildfires, which are uncontrolled fires spreading rapidly across natural landscapes, are significantly influenced by meteorological conditions (He et al., 2019; Jones et al., 2022). In Australia, these fires, also known as bushfires, present a major environmental and social threat (Johnston et al., 2021; Ward et al., 2020). According to Dowdy (2020), the most favorable seasons for wildfires in most regions of Australia are austral spring and summer. Key meteorological factors such as extended periods of drought, elevated temperatures, low humidity, and strong winds are crucial in determining the occurrence and intensity of wildfires (Zacharakis and Tsihrintzis, 2023). Under the recent historical climate change, Australia has witnessed a rise in extreme fire weather conditions and an extended fire season (CSIRO and BOM, 2022).

Since the implementation of clean air policies in 2013, there has been a noticeable decrease in aerosol levels in China (Zhang et al., 2019; Zheng et al., 2018). Numerous studies have shown the local and global climate effects of the aerosol reductions in China (Dang and Liao, 2019; Gao et al., 2022, 2023; Liu et al., 2023; Zheng et al., 2020). The Australian monsoonal wind patterns, reported to be influenced by Asian aerosol emissions in the past decades (Rotstayn et al., 2007; Fahrenbach et al., 2023), may have also influenced by the radiative effects due to the aerosol decline in China. The objective of this study is to assess the worsened dry and warm conditions and associated wildfire risk in Australia during 2013–2019 and investigate the possible linkage between the changes in climate conditions in Australia and anthropogenic aerosols.

2 Methods

2.1 Observational and Reanalysis Data

Ground-based observational data of near-surface PM_{2.5} concentrations in China 2013–2019

are acquired from the China National Environmental Monitoring Centre (CNEMC), which offers daily records of near-surface air pollutant concentrations for nearly 1800 sites. Aerosol Optical Depth (AOD) data are obtained from the Moderate Resolution Imaging Spectroradiometer (MODIS) Deep Blue retrieval (Hsu et al., 2013). These observational data are used for evaluating the performance of model simulated aerosols.

ERA5, the fifth generation of the European Centre for Medium-range Weather Forecasts (ECMWF) atmospheric reanalysis, is a comprehensive dataset that provides a detailed and globally consistent view of the earth's atmospheric conditions over the past several decades (Hersbach et al., 2020). In this study, ERA5 data are employed to evaluate the climate condition in Australia and analyze its linkage with aerosol reductions in China during the 2013–2019 by using the 2-meter temperature, total precipitation, relative humidity, cloud cover, wind fields, vertical velocity, surface latent and sensible heat flux, and surface and top of the atmosphere (TOA) solar and longwave radiative flux under both clear and all sky conditions.

Clouds and the Earth's Radiant Energy System-Energy Balanced and Filled (CERES-EBAF) is a dataset that provides information on the earth's radiation budget, including surface and TOA energy fluxes (Loeb et al., 2018). It combines data from satellite instruments to estimate how much energy the earth receives from the sun and how much is reflected back to space, helping to understand climate change and energy balance processes. The variables used in the study include cloud cover and surface and TOA solar and longwave radiative fluxes under both clear and all sky conditions.

The Global Precipitation Measurement (GPM) mission is a joint initiative by National Aeronautics and Space Administration (NASA) and the Japan Aerospace Exploration Agency (JAXA) aimed at providing accurate and frequent measurements of global precipitation (Skofronick-Jackson et al., 2017). GPM includes a core satellite equipped with advanced radar and microwave sensors, enabling the observation of rain and snowfall in real-time. The data are crucial for understanding weather patterns, climate dynamics, and hydrological processes. Precipitation rate data from GPM are also used in the study. GPM provides higher temporal and spatial resolution data compared to Global Precipitation Climatology Project (GPCP), making it more suitable for studies focused on short-term precipitation variability and regional climate dynamics.

2.2 Model Description and Experimental Design

In this research, we conduct simulations to explore the impact of aerosols on climate using the Community Earth System Model version 1 (CESM1). CESM1 simulates the major aerosols including sulfate, black carbon (BC), primary organic matter (POM), secondary organic aerosol (SOA), dust and sea salt in a four-mode Modal Aerosol Module (MAM4), as described in Liu et al. (2016). CESM1 simulations are carried out with 30 vertical layers and a horizontal resolution of 2.5° longitude by 1.9° latitude. In addition to the default model physics, several supplementary features are incorporated into the model in this study to improve the model's performance in simulating aerosol wet scavenging and convective transport (Wang et al., 2013).

The global anthropogenic emissions of aerosols and their precursors are obtained from the Community Emissions Data System (CEDS) v_2021_04_21. In contrast to the prior CEDS v_2016_07_26, which exhibits significant regional emission biases (Z. Wang et al., 2021), the newer CEDS version of anthropogenic emissions of aerosols and precursors considers the substantial reductions in emissions in China, related to the recent clean air actions since 2013 (Fig. S1). Specifically, anthropogenic sulfur dioxide (SO_2), BC, and organic carbon (OC) emissions decreased by -12.48 , -0.30 , and -0.21 Tg yr^{-1} , respectively, over China between 2013 and 2019. Biogenic emissions are from the Model of Emissions of Gases and Aerosols from Nature version 2.1 (MEGAN v2.1) (Guenther et al., 2012), while the emissions from open biomass burning are derived from the CMIP6 (Coupled Model Intercomparison Project Phase 6) (Van Marle et al., 2017).

A series of model experiments are conducted using CESM1 with a fully-coupled model configuration, as detailed in Table S1. In the baseline scenario (referred to as BASE), anthropogenic emissions of aerosols and precursors are fixed at year 2013 worldwide. In CHN, anthropogenic emissions of aerosols and precursors over China are fixed at year 2019, while emissions in all other regions are remained at year 2013. In NAEU, the simulation is performed with anthropogenic emissions of aerosols and precursors over North America and Europe set at year 2019, while emissions in other regions remained at year 2013. In OTH, anthropogenic emissions of aerosols and precursors in other regions except for China are set at year 2019, while emissions in China are kept at year 2013. Biogenic and biomass burning emissions worldwide in

all experiments are fixed at year 2013. To reduce model biases related to internal variability, three ensemble members are conducted by perturbing the initial atmospheric temperature conditions. All simulations are run for 150 years, with the last 100 years for detailed analysis.

2.3 Model Evaluation

To validate whether CESM1 can reproduce the aerosol reductions in China during the 2010s, changes in simulated near-surface $\text{PM}_{2.5}$ concentrations (sum of sulfate, BC, POM, SOA, dust $\times 0.1$, and sea-salt $\times 0.25$ following Turnock et al. (2020)) in China during 2013–2019 are compared with the observations. Figure S2 shows spatial distributions of observed and modeled annual mean near-surface $\text{PM}_{2.5}$ concentration changes over China (2017–2019 minus 2013–2015), which exhibited a statistically significant correlation coefficient of 0.52 between simulations and observations. However, the model underestimates the $\text{PM}_{2.5}$ concentration changes by 76% in China. The considerable underestimation has been reported in many previous studies, resulting from coarse model resolution, uncertainties in emissions of aerosols and precursor gases, strong aerosol wet removal, and the model's deficiency in simulating nitrate and ammonium aerosols (Fan et al., 2018, 2022; Gao et al., 2022, 2023; Zeng et al., 2021). The model has a good capability in replicating the spatial distribution of AOD changes in China during 2013–2019 (Fig. S3), as evidenced by a high correlation coefficient of 0.83, but the model also exhibits an underestimation in the AOD reductions by 69%.

Climate variables, including precipitation rate, surface air temperature, relative humidity, total cloud cover, surface solar radiation, 10m wind speed, and surface and TOA net total radiative fluxes under both clear and all sky conditions over Australia simulated by CESM1 model are also compared with those from ERA5 reanalysis (Fig. S4–S6). The model demonstrates a good performance in simulating Australian climate, with normalized mean bias (NMB) values consistently below or near 40% for surface air temperature, relative humidity, total cloud cover, surface downward solar radiation, and 10m wind speed, and surface and TOA net total radiative fluxes, but it tends to overestimate annual precipitation by about 90%, especially over coastal regions likely related to the coarse model resolution. The model accurately reproduces spatial patterns of all climate variables, closely aligning with observations, as indicated by correlation coefficients ranging from 0.7 to 1.0.

2.4 Wildfire Risk Indices

In this study, several climatological indices are used to indicate wildfire risk during fire seasons (austral spring and summer, from September to February of the next year) in Australia (Ren et al., 2022; Irmak et al., 2003; Seager et al., 2015; Sharples et al., 2009).

(i) Reference Potential Evapotranspiration (ET_0):

ET_0 is a climatological index used to estimate the amount of water that could potentially evaporate and be transpired from the ~~earth's~~Earth's surface under specific meteorological conditions. The calculation of ET_0 takes into account factors such as temperature (T , unit: $^{\circ}\text{C}$), and surface downward solar radiation (R_s , unit: W m^{-2}) to estimate the maximum amount of water loss due to evaporation and transpiration. ET_0 is important in wildfire studies because it helps to gauge the environmental moisture conditions and the potential for drought, which can be a significant factor in wildfire risks assessment. ET_0 is given by the following expression (Irmak et al., 2003):

$$ET_0 = -0.611 + 0.149R_s + 0.079T$$

(ii) Vapor Pressure Deficit (VPD):

Vapor Pressure Deficit (VPD) is a meteorological parameter that measures the difference between the amount of moisture in the air and the maximum amount of moisture the air can hold at a given temperature (T , unit: $^{\circ}\text{C}$) and moisture (relative humidity, RH , unit: %). High VPD values indicate that the air is dry. VPD is important in the context of wildfires because it reflects the drying potential of the atmosphere. When VPD is high, it can lead to rapid moisture loss from vegetation, making it more susceptible to ignition and increasing the risk of wildfires. VPD is given by (Seager et al., 2015):

$$VPD = \frac{100 - RH}{100} \times 610.7 \times 10^{\frac{7.5T}{237.3+T}}$$

(iii) McArthur Forest Fire Danger Index (FFDI):

The McArthur Forest Fire Danger Index (FFDI) is a widely used index in Australia to assess the potential for bushfires and forest fires. It takes into account various meteorological factors,

including T (unit: °C), RH (unit: %), wind speed (U, unit: m s⁻¹), and drought factor (DF, unitless). We set DF as 10 here following Sharples et al. (2009), as it would not significantly affect the methods of comparison used later in their study. While we acknowledge that this assumption is idealized, we find it applicable in our case. To verify this, we calculated gridded DFs for Australia (Figure S7), which show that the DFs are close to 10 and exhibit nearly homogeneous spatial distributions. As such, setting DF = 10 for Australia is reasonable for our analysis. In addition, FFDI calculated using DF = 10 and FFDI using gridded DFs are compared (Figure S8). The patterns and regional averages of both datasets are very similar, further supporting the use of DF = 10 in our study. The FFDI provides a numerical rating that indicates the level of fire danger, with higher values corresponding to greater fire risks. This index is particularly valuable for assessing the immediate risk of wildfires and is commonly used in fire management and prediction. FFDI is defined as (Sharples et al., 2009):

$$FFDI = 2e^{-0.45+0.987\ln DF+0.0338T-0.0345RH+0.0234U}$$

3 Results

3.1 Intensified Dry and Warm Conditions in Australia by aerosol changes

Figure 1 shows simulated responses in annual ~~and seasonal~~ precipitation rate, surface air temperature and relative humidity in Australia to changes in anthropogenic emissions of aerosols and precursors ~~in China~~. In response to aerosol reductions in China, Australia experiences significant decreases in precipitation and relative humidity, while the temperature has an increase from 2013 to 2019. On regional average, annual precipitation, surface air temperature and relative humidity change by -0.10 mm day⁻¹, 0.08 °C, and -1.19%, respectively, in Australia caused by the aerosol reduction in China during this time period, contributing to the dry and warm climate in Australia. Notably, Northern Australia experiences the most significant reduction in convective precipitation, whereas Southern Australia has the greatest decline in large-scale precipitation related to the aerosol reduction in China, as simulated by the CESM1 model (Fig. S7S9). The direction of seasonal responses in precipitation rate, surface air temperature and relative humidity are the same as the annual averages, with the largest changes occurring in austral spring (Fig. 42).

The intensified dry and warm conditions in Australia can also be seen in the observations, as indicated by ERA5 reanalysis data (Fig. 23). Since 2010, precipitation and relative humidity have significantly decreased in Australia, especially in Northern and Eastern Australia, at a rate of $0.086 \text{ mm day}^{-1} \text{ yr}^{-1}$ and $1.07\% \text{ yr}^{-1}$, respectively, while surface air temperature has increased at a rate of $0.17 \text{ }^{\circ}\text{C yr}^{-1}$. Note that, the trends in observations are calculated during 2010–2019 to minimize the internal variability. The decrease in precipitation in Australia is also reflected in the GPM data (Fig. S8S10). It translates into the changes in precipitation, temperature and relative humidity by 0.52 mm day^{-1} , $1.0 \text{ }^{\circ}\text{C}$ and 6.4% in Australia during 2013–2019 in observations if the trends are assumed to be linear. This suggests that aerosol reductions in China can explain 19% of the decreases in precipitation and relative humidity and 8% of the increase in surface air temperature in Australia during 2013–2019, worsening the dry and warm climate conditions in Australia (Fig. S9). S11). However, considering that aerosols are underestimated in the model, the impact of aerosol reductions in China on Australia’s climate may also be underestimated. The reduction in anthropogenic SO_2 emissions in China shows strong correlations with the decrease in precipitation and the increase in temperature in Australia during 2010–2019 (Fig. S40S12). However, when extending the time frame to the period before emissions reductions in China (1940–2019), the increase in temperature becomes less pronounced, with a slight rise in precipitation and relative humidity, likely attributed to greenhouse gas warming, which can serve as evidenc that the decrease in precipitation and increase in temperature in Australia from 2010 to 2019 are not primarily caused by GHGs (Figure S44S13). The rainfall decrease is consistent with changes in clouds. Spatial distributions of simulated changes in vertically-integrated cloud cover and the linear trends in observations are shown in Fig. S12–S14–S16. In both observation and model simulation, the results consistently indicate a reduction in clouds of all levels, including high, mid-level, and low clouds. In addition, the spatial distributions of these changes closely resemble the patterns of responses in precipitation and relative humidity.

Aerosol emissions have changed across the world rather than in China alone during 2013–2019, such as those in Australia, North America and Europe, which affect climate in both local and remote regions. ~~Figures S15a and S15b~~ Figure 1 also shows changes in ~~precipitation and surface temperature~~ climate variables in Australia due to changes in other regions except China. The aerosol changes in other regions except China yield a decrease in precipitation by 0.05 mm day^{-1} ~~and,~~ an increase in temperature by $0.08 \text{ }^{\circ}\text{C}$, ~~which are similar to those caused and a decrease~~

in relative humidity by ~~the aerosol changes in China (Fig. 1)~~ 0.67%. In particular, North America and Europe emission changes ~~largely, to some extent,~~ contribute to the responses in precipitation ($-0.04 \text{ mm day}^{-1}$) ~~and~~, temperature ($0.08 \text{ }^{\circ}\text{C}$) and relative humidity (-0.33%) attributed to other regions (except China), although the responses are mostly insignificant (~~Figs. 15c and 15d~~ Fig. 1).

3.2 Mechanisms of Dry and Warm conditions in Australia Amplified by Aerosol Reductions in China

The rising levels of Asian aerosols could influence the meridional temperature and pressure gradients across the Indian Ocean and therefore affect monsoonal winds and rainfall in Australia since the middle of the 20th century, as reported in several previous studies (Fahrenbach et al., 2023; Rotstayn et al., 2007). Since 2013, aerosol levels in China have substantially decreased due to clean air actions initiated by the Chinese government (Zhang et al., 2019). At the same time, precipitation in Australia exhibited a declining trend, which could be partly attributed to the decrease in China's anthropogenic aerosol forcing as quantified through CESM1 simulations.

Asian monsoon region is closely connected with the meridional Hadley circulation and zonal Walker circulation through monsoon outflow to the South India ocean subtropical high (SISH) and North Pacific subtropical high (NPSH) (Beck et al., 2018). Figure ~~S164a~~ S174a illustrates the climatological mean wind fields at 850 hPa, indicating the persistent existence of SISH in the Indian Ocean and NPSH in the North Pacific. With reductions in aerosols in China, the sea surface temperature (SST) increases in the North Pacific but decreases in the Indian Ocean (Fig. ~~S174b~~ S174b), which is concurrent with the northward shift of the Intertropical Convergence Zone (ITCZ) (Basha et al., 2015). Over Asia, this migration of ITCZ is accompanied by the northward movement of the upper-tropospheric subtropical zonal westerly jet (Chiang et al., 2015; Schiemann et al., 2009), which moves to the north of the Tibetan Plateau. It then enhances the circulation pattern of the Tibetan high, redirects the outflow from the Asian monsoon to the southern Indian Ocean subtropical high (Fig. ~~3e5c~~ 3e5c), strengthens the SISH, and leads to the enhancement of the Southern Trade Winds (Fig. ~~3d5d~~ 3d5d). On the other hand, the increase in SST in the North Pacific induces ascending motion around the 130° – 150°E and the subsequent descending motion around the 90° – 110°E (Fig. ~~3b5b~~ 3b5b), with anomalous westerly winds near the surface, leading to a weakening of NPSH along with a decrease in the Northern Trade Winds (Fig. ~~3d5d~~ 3d5d). Note that, the descending

650 motion partly compensates the ascending motion related to the meridional circulation between
651 10°–30°N (Fig. 3e). ~~Similar changes of vertical and horizontal circulations are also shown in the~~
652 ~~real world in the 2010s (Fig. S18).5c). Although only a few significant changes persist in Northern~~
653 ~~Australia, the observed large-scale circulations around Australia show noticeable similarities to~~
654 ~~the simulated results (Fig. S17). The mechanism of China's aerosol reductions on the large-scale~~
655 ~~3D circulation in the Asia-Pacific region is shown in Figure 6.~~ The enhancement of the Southern
656 Trade Winds further causes moisture advection away from Australia, accompanied by moisture
657 divergence in Australia, especially over the northern Australia (Fig. S19S18). Moisture divergence
658 is also evident in the observations for some northern regions of Australia (Fig. S20S19). This
659 moisture divergence in Australia then intensifies the dryness in Australia both in CESM1
660 simulations (Fig. 1) and ERA5 reanalysis (Fig. 23).

661 Figures S247 illustrate the changes in relevant radiative fluxes in Australia resulting from
662 aerosol changes in China. Under the clear sky condition, both surface and top of the atmosphere
663 (TOA) radiative flux decrease (Fig. S24e7c&d). It is due to increased sea salt and dust aerosols
664 (Fig. S22bS20b–d) due to the stronger Southern Trade Winds (Figs. S22aS20a and 3d5d) and dryer
665 conditions (Fig. 4a&e1). The decrease in cloud cover (Fig. S12S14) leads to an overall increase in
666 both surface and TOA radiative flux (Fig. S24e7e&f). The overall changes in radiative fluxes are
667 offset by these two factors (Fig. S24a7a&b) and insufficient to explain the significant increase in
668 surface air temperature in Australia (Fig. 4b1). Similar signals are also evident in the observational
669 data represented by ERA5 and CERES-EBAF (Figs. S23S21 and S24S22).

670 Decreases in precipitation lead to a decrease in surface specific humidity (Fig. S25aS23a),
671 which declines more than that at 850 hPa (Fig. S25bS23b). This results in excess energy being
672 converted into sensible heat rather than latent heat through evaporation (Chiang et al., 2018;
673 Fischer et al., 2007; Seneviratne et al., 2006; Su et al., 2014), which is indicated by a decrease in
674 surface upward latent heat flux and an increase in surface upward sensible heat flux in Australia
675 due to aerosol changes in China in Figure S268. The increased surface upward sensible heat flux
676 heats the near-surface air and contributes to the warm conditions in Australia. The signals of
677 specific humidity and surface sensible/latent heat flux from ERA5 are consistent with the
678 simulated results. (Figs. S27S24 and S28S25).

3.3 Increases in Wildfire Risk in Australia

Wildfires represent a biosphere-atmosphere phenomenon, arising from the intricate interplay of weather, climate, fuels, and human activities (Moritz et al., 2014). Notably, wildfires are ranked among the most significant natural disasters in Australia, causing extensive damage (Shi et al., 2021). Collins et al. (2022) reported that warmer and drier conditions increased the potential for large and severe wildfire in Australia. Given that changes in aerosols in China have led to a warmer and drier climate condition in Australia in recent years, the change in this climate state could also impact on the occurrence of wildfires. Three wildfire risk indices (ET_0 , VPD, and FFDI) are selected to assess the risks of wildfires occurrence. Detailed information about the three wildfire risk indices can be found in the Methods section.

All three indices exhibit increases ($+0.36 \text{ mm mon}^{-1}$ for ET_0 , $+0.56 \text{ hPa}$ for VPD, and $+0.24$ for FFDI) during fire seasons (September to February) in Australia due to changes in aerosols in China during 2013–2019 (Fig. 49), although they do not show the same spatial distribution possibly due to different considerations regarding climate variables in the indices. The results analyzed from observational data also exhibit increasing trends at a rate of $0.32 \text{ mm mon}^{-1} \text{ yr}^{-1}$ for ET_0 , 0.59 hPa yr^{-1} for VPD, and 0.34 yr^{-1} for FFDI during this time period (Fig. S29S26). It further indicates that the decline in anthropogenic aerosols in China can explain 12%–19% of the increase in wildfire risks during the fire season in Australia between 2013 and 2019 through inducing dry and warm wildfire weather conditions (Fig. S9). However, considering that aerosols are underestimated in the model, the impact of aerosol reductions in China on Australia's wildfire risks may also be underestimated.

4 Conclusions and Discussions

This study reveals a plausible connection between the substantial aerosol reduction in China and drying and warming trends in Australia that happened during the 2010s. Aerosol reductions in China induce changes in temperature and pressure gradients, which lead to an increased outflow from Asia towards the South Indian Ocean, strengthening the SISH and the associated Southern Trade Winds. Consequently, this atmospheric pattern results in moisture divergence over Australia, causing a decrease in humidity and precipitation. The reduction in surface moisture leads to more surface energy being converted into sensible heat, rather than evaporating as latent heat, thereby

heating the near-surface air. This perspective sheds light on the influence of distant aerosols on climate in Australia.

The CESM1 simulations depict warmer and drier conditions in Australia related to China's aerosol reductions than otherwise, a pattern also evident in observations represented by ERA5. However, it is important to note that China's aerosol reductions only contribute to a portion of the observed warm and dry conditions in Australia. According to the CESM1 simulations, aerosol changes in China account for 19% of the observed decrease in relative humidity and precipitation and 8% of the increase in temperature in Australia throughout the year, and 12%–19% of the increase in wildfire risks during the fire season in Australia during 2013–2019. Given that aerosols are underestimated in the model, the effect of aerosol reductions in China on Australia's climate and wildfire risks might also be underestimated. Nonetheless, air quality and human health improvements owing to aerosol reductions cannot be ignored (Giani et al., 2020; Zheng et al., 2017). In addition, the drying and warming trends in Australia attributed to aerosol reductions should be considered resulting from the rise in long-lived GHGs, while the aerosol reductions unmask the effect rooted in the GHGs (Wang et al., 2023). In addition, other factors such as internal climate variability (Heidemann et al., 2023) appear to have contributed more to the changes in Australia's climate conditions.

There are some potential limitations and uncertainties in this study. Firstly, the low bias in simulated aerosol concentrations in CESM1 could potentially lead to an underestimation of the climate responses in Australia, and the extent to which the low bias could influence the results remains unknown. Secondly, our findings are derived from simulations conducted with a single aerosol-fully-coupled climate model, and it is vital for future research to employ multi-model ensemble simulations to reduce the possibility of model-dependent specific results. While the CMIP6 and PDRMIP (Precipitation Driver Response Model Intercomparison Project) can assist in minimizing such model dependencies, they also present certain drawbacks. Anthropogenic emissions input in CMIP6 inadequately accounts for aerosol reductions resulting from clean air actions in China since 2013 (Z. Wang et al., 2021). Additionally, CMIP6 considers aerosol changes globally, making it challenging to isolate effects specifically induced by changes in aerosols in China. The experimental design of PDRMIP, which scales the concentrations of sulfate and BC in Asia to ten times of their present-day levels, is generally idealistic and may not accurately and

proportionally represent aerosol changes observed in the real world. Until now, few studies have explored the link between the recent reduction in China's aerosols and the changing climate conditions in Australia. Although Fahrenbach et al. (2023) investigated the connection between increased precipitation in Australia and elevated aerosol levels in Asia since the last century, they focused on the decadal time scale with historical increasing aerosols in Asia. Besides, while this study relies on equilibrium simulations to isolate the forced response to aerosol changes, we acknowledge that transient simulations, which account for time-varying aerosol reductions, would provide a more accurate depiction of the dynamic climate system response. Given that aerosol reductions in China continue to evolve, transient simulations would be more appropriate for capturing the full temporal effects of these changes. Large-ensemble transient simulations are suggested in future studies to better represent the evolving aerosol-climate interactions over time and to enhance the robustness of the findings. Another limitation of this study is that we calculated the relative contribution of aerosol changes in China to the changing climate in Australia by combining model simulations and observational data, which could lead to the inconsistency and introduce biases to the quantitative results. Finally, in addition to aerosols, GHGs also contribute to regional and global climate change. The extent to which GHGs could contribute to weather condition and climate changes in Australia remains unknown, which warrants further investigation.

Nonetheless, our study examined the role of China's aerosol reductions in Australia's recent drying and warming trends. Substantial emission reductions will continue in China following the carbon neutral pathway (Yang et al., 2023), while future changes in emissions in South Asia remain uncertain (Samset et al., 2019). Apart from natural climate variabilities that affect the Australian monsoon, further investigation of changes in monsoon precipitation in Australia should also consider the effects of remote aerosol changes simultaneously, which is crucial to effective drought and wildfire management and mitigation in Australia.

Acknowledgments

This study was supported by the National Natural Science Foundation of China (grant no. 42475032), the Jiangsu Science Fund for Carbon Neutrality (grant no. BK20220031), and Jiangsu Innovation and Entrepreneurship Team (grant no. JSSCTD202346). H.W. acknowledges the support of the U.S. Department of Energy (DOE), Office of Science, Office of Biological and

Environmental Research (BER), as part of the Earth and Environmental System Modeling program. The Pacific Northwest National Laboratory (PNNL) is operated for DOE by the Battelle Memorial Institute under contract DE-AC05-76RLO1830.

Data and Code Availability

Ground-based observed PM_{2.5} concentrations from CNEMC are available at <https://quotsoft.net/air/> (last access: September 2024). AOD from MODIS Deep Blue retrieval are available at <https://modis.gsfc.nasa.gov/> (last access: September 2024). ERA5 reanalysis data are available at <https://cds.climate.copernicus.eu/> (last access: September 2024). CERES-EBAF data are available at <https://ceres.larc.nasa.gov/data/#energy-balanced-and-filled-ebaf> (last access: September 2024). GPM data are available at https://disc.gsfc.nasa.gov/datasets/GPM_3IMERGM_07/summary?keywords=%22IMERGM%20final%22 (last access: September 2024). The source code of CESM is available at <https://github.com/ESCOMP/CESM> (last access: September 2024). Our model results can be available at <https://doi.org/10.5281/zenodo.13682943> (last access: September 2024).

Author Contributions

Y.Y. conceived the research and directed the analysis. J.G. conceived the research, conducted the model simulations, and performed the analysis. All the authors including H.W., P.W., and H. L. discussed the results and wrote the paper.

Competing Interests

At least one of the (co-)authors is a member of the editorial board of Atmospheric Chemistry and Physics. The peer-review process was guided by an independent editor, and the authors also have no other competing interests to declare.

References

Basha, G., Kishore, P., Venkat Ratnam, M., Ouarda, T. B. M. J., Velicogna, I., and Sutterley, T.: Vertical and latitudinal variation of the intertropical convergence zone derived using GPS radio occultation measurements, Remote Sens. Environ., 163, 262–269, <https://doi.org/10.1016/j.rse.2015.03.024>, 2015.

- Beck, J. W., Zhou, W., Li, C., Wu, Z., White, L., Xian, F., Kong, X., and An, Z.: A 550,000-year record of East Asian monsoon rainfall from 10Be in loess, *Science*, 360, 877–881, <https://doi.org/10.1126/science.aam5825>, 2018.
- Boer, M. M., Resco De Dios, V., and Bradstock, R. A.: Unprecedented burn area of Australian mega forest fires, *Nat. Clim. Change*, 10, 171–172, <https://doi.org/10.1038/s41558-020-0716-1>, 2020.
- Bollasina, M. A., Ming, Y., and Ramaswamy, V.: Anthropogenic Aerosols and the Weakening of the South Asian Summer Monsoon, *Science*, 334, 502–505, <https://doi.org/10.1126/science.1204994>, 2011.
- Bollasina, M. A., Ming, Y., Ramaswamy, V., Schwarzkopf, M. D., and Naik, V.: Contribution of local and remote anthropogenic aerosols to the twentieth century weakening of the South Asian Monsoon, *Geophys. Res. Lett.*, 41, 680–687, <https://doi.org/10.1002/2013GL058183>, 2014.
- Chiang, F., Mazdiyasni, O., and AghaKouchak, A.: Amplified warming of droughts in southern United States in observations and model simulations, *Sci. Adv.*, 4, eaat2380, <https://doi.org/10.1126/sciadv.aat2380>, 2018.
- Chiang, J. C. H., Fung, I. Y., Wu, C.-H., Cai, Y., Edman, J. P., Liu, Y., Day, J. A., Bhattacharya, T., Mondal, Y., and Labrousse, C. A.: Role of seasonal transitions and westerly jets in East Asian paleoclimate, *Quat. Sci. Rev.*, 108, 111–129, <https://doi.org/10.1016/j.quascirev.2014.11.009>, 2015.
- Collins, L., Clarke, H., Clarke, M. F., McColl Gausden, S. C., Nolan, R. H., Penman, T., and Bradstock, R.: Warmer and drier conditions have increased the potential for large and severe fire seasons across south-eastern Australia, *Glob. Ecol. Biogeogr.*, 31, 1933–1948, <https://doi.org/10.1111/geb.13514>, 2022.
- Cook, B. I. and Seager, R.: The response of the North American Monsoon to increased greenhouse gas forcing, *J. Geophys. Res.: Atmos.*, 118, 1690–1699, <https://doi.org/10.1002/jgrd.50111>, 2013.
- Cowan, T. and Cai, W.: The impact of Asian and non-Asian anthropogenic aerosols on 20th century Asian summer monsoon: ASIAN MONSOON AND AEROSOLS, *Geophys. Res. Lett.*, 38, L11703, <https://doi.org/10.1029/2011GL047268>, 2011.
- CSIRO and BOM: State of the Climate 2022, 2022
- Dang, R. and Liao, H.: Radiative Forcing and Health Impact of Aerosols and Ozone in China as the Consequence of Clean Air Actions over 2012–2017, *Geophys. Res. Lett.*, 46, 12511–12519, <https://doi.org/10.1029/2019GL084605>, 2019.
- Dey, R., Lewis, S. C., Arblaster, J. M., and Abram, N. J.: A review of past and projected changes in Australia’s rainfall, *WIREs Clim. Change*, 10, e577, <https://doi.org/10.1002/wcc.577>, 2019a.

- Dey, R., Lewis, S. C., and Abram, N. J.: Investigating observed northwest Australian rainfall trends in Coupled Model Intercomparison Project phase 5 detection and attribution experiments, *Int. J. Climatol.*, 39, 112–127, <https://doi.org/10.1002/joc.5788>, 2019b.
- Dong, B., Wilcox, L. J., Highwood, E. J., and Sutton, R. T.: Impacts of recent decadal changes in Asian aerosols on the East Asian summer monsoon: roles of aerosol–radiation and aerosol–cloud interactions, *Clim. Dyn.*, 53, 3235–3256, <https://doi.org/10.1007/s00382-019-04698-0>, 2019.
- Dowdy, A. J.: Seamless climate change projections and seasonal predictions for bushfires in Australia, *J. South. Hemisph. Earth Syst. Sci.*, 70, 120–138, <https://doi.org/10.1071/ES20001>, 2020.
- Evans, S., Marchand, R., and Ackerman, T.: Variability of the Australian Monsoon and Precipitation Trends at Darwin, *J. Climate*, 27, 8487–8500, <https://doi.org/10.1175/JCLI-D-13-00422.1>, 2014.
- Fahrenbach, N. L. S., Bollasina, M. A., Samset, B. H., Cowan, T., and Ekman, A. M. L.: Asian anthropogenic aerosol forcing played a key role in the multi-decadal increase in Australian summer monsoon rainfall, *J. Climate*, 1, <https://doi.org/10.1175/JCLI-D-23-0313.1>, 2023.
- Fan, T., Liu, X., Ma, P.-L., Zhang, Q., Li, Z., Jiang, Y., Zhang, F., Zhao, C., Yang, X., Wu, F., and Wang, Y.: Emission or atmospheric processes? An attempt to attribute the source of large bias of aerosols in eastern China simulated by global climate models, *Atmos. Chem. Phys.*, 18, 1395–1417, <https://doi.org/10.5194/acp-18-1395-2018>, 2018.
- Fan, T., Liu, X., Wu, C., Zhang, Q., Zhao, C., Yang, X., and Li, Y.: Comparison of the Anthropogenic Emission Inventory for CMIP6 Models with a Country-Level Inventory over China and the Simulations of the Aerosol Properties, *Adv. Atmos. Sci.*, 39, 80–96, <https://doi.org/10.1007/s00376-021-1119-6>, 2022.
- Fischer, E. M., Seneviratne, S. I., Lüthi, D., and Schär, C.: Contribution of land-atmosphere coupling to recent European summer heat waves, *Geophys. Res. Lett.*, 34, 2006GL029068, <https://doi.org/10.1029/2006GL029068>, 2007.
- Gao, J., Yang, Y., Wang, H., Wang, P., Li, H., Li, M., Ren, L., Yue, X., and Liao, H.: Fast climate responses to emission reductions in aerosol and ozone precursors in China during 2013–2017, *Atmos. Chem. Phys.*, 22, 7131–7142, <https://doi.org/10.5194/acp-22-7131-2022>, 2022.
- Gao, J., Yang, Y., Wang, H., Wang, P., Li, B., Li, J., Wei, J., Gao, M., and Liao, H.: Climate responses in China to domestic and foreign aerosol changes due to clean air actions during 2013–2019, *npj Clim. Atmos. Sci.*, 6, 160, <https://doi.org/10.1038/s41612-023-00488-y>, 2023.
- Giani, P., Castruccio, S., Anav, A., Howard, D., Hu, W., and Crippa, P.: Short-term and long-term health impacts of air pollution reductions from COVID-19 lockdowns in China and Europe:

- a modelling study, *Lancet Planet. Health*, 4, e474–e482, [https://doi.org/10.1016/S2542-5196\(20\)30224-2](https://doi.org/10.1016/S2542-5196(20)30224-2), 2020.
- Guenther, A. B., Jiang, X., Heald, C. L., Sakulyanontvittaya, T., Duhl, T., Emmons, L. K., and Wang, X.: The Model of Emissions of Gases and Aerosols from Nature version 2.1 (MEGAN2.1): an extended and updated framework for modeling biogenic emissions, *Geosci. Model Dev.*, 5, 1471–1492, <https://doi.org/10.5194/gmd-5-1471-2012>, 2012.
- He, T., Lamont, B. B., and Pausas, J. G.: Fire as a key driver of Earth’s biodiversity, *Biol. Rev.*, 94, 1983–2010, <https://doi.org/10.1111/brv.12544>, 2019.
- Head, L., Adams, M., McGregor, H. V., and Toole, S.: Climate change and Australia, *WIREs Clim. Change*, 5, 175–197, <https://doi.org/10.1002/wcc.255>, 2014.
- Heidemann, H., Cowan, T., Henley, B. J., Ribbe, J., Freund, M., and Power, S.: Variability and long-term change in Australian monsoon rainfall: A review, *WIREs Clim. Change*, 14, e823, <https://doi.org/10.1002/wcc.823>, 2023.
- Hersbach, H., Bell, B., Berrisford, P., Hirahara, S., Horányi, A., Muñoz-Sabater, J., Nicolas, J., Peubey, C., Radu, R., Schepers, D., Simmons, A., Soci, C., Abdalla, S., Abellan, X., Balsamo, G., Bechtold, P., Biavati, G., Bidlot, J., Bonavita, M., De Chiara, G., Dahlgren, P., Dee, D., Diamantakis, M., Dragani, R., Flemming, J., Forbes, R., Fuentes, M., Geer, A., Haimberger, L., Healy, S., Hogan, R. J., Hólm, E., Janisková, M., Keeley, S., Laloyaux, P., Lopez, P., Lupu, C., Radnoti, G., De Rosnay, P., Rozum, I., Vamborg, F., Villaume, S., and Thépaut, J.: The ERA5 global reanalysis, *Q. J. R. Meteorol. Soc.*, 146, 1999–2049, <https://doi.org/10.1002/qj.3803>, 2020.
- Hoesly, R. M., Smith, S. J., Feng, L., Klimont, Z., Janssens-Maenhout, G., Pitkanen, T., Seibert, J. J., Vu, L., Andres, R. J., Bolt, R. M., Bond, T. C., Dawidowski, L., Kholod, N., Kurokawa, J., Li, M., Liu, L., Lu, Z., Moura, M. C. P., O’Rourke, P. R., and Zhang, Q.: Historical (1750–2014) anthropogenic emissions of reactive gases and aerosols from the Community Emissions Data System (CEDS), *Geosci. Model Dev.*, 11, 369–408, <https://doi.org/10.5194/gmd-11-369-2018>, 2018.
- Hsu, N. C., Jeong, M. -J., Bettenhausen, C., Sayer, A. M., Hansell, R., Seftor, C. S., Huang, J., and Tsay, S. -C.: Enhanced Deep Blue aerosol retrieval algorithm: The second generation, *J. Geophys. Res.: Atmos.*, 118, 9296–9315, <https://doi.org/10.1002/jgrd.50712>, 2013.
- Huneus, N., Denier Van Der Gon, H., Castesana, P., Menares, C., Granier, C., Granier, L., Alonso, M., De Fatima Andrade, M., Dawidowski, L., Gallardo, L., Gomez, D., Klimont, Z., Janssens-Maenhout, G., Osses, M., Puliafito, S. E., Rojas, N., Ccoyllo, O. S., Tolvett, S., and Ynoue, R. Y.: Evaluation of anthropogenic air pollutant emission inventories for South America at national and city scale, *Atmos. Environ.*, 235, 117606, <https://doi.org/10.1016/j.atmosenv.2020.117606>, 2020.
- IPCC: Climate Change 2013: The Physical Science Basis, 2013.
- IPCC: Climate Change 2021: The Physical Science Basis, 2021.

906 Irmak, S., Irmak, A., Allen, R. G., and Jones, J. W.: Solar and Net Radiation-Based Equations to
 907 Estimate Reference Evapotranspiration in Humid Climates, *J. Irrig. Drain. Eng.*, 129, 336–
 908 347, [https://doi.org/10.1061/\(ASCE\)0733-9437\(2003\)129:5\(336\)](https://doi.org/10.1061/(ASCE)0733-9437(2003)129:5(336)), 2003.

909 Johnston, F. H., Borchers-Arriagada, N., Morgan, G. G., Jalaludin, B., Palmer, A. J., Williamson,
 910 G. J., and Bowman, D. M. J. S.: Unprecedented health costs of smoke-related PM_{2.5} from
 911 the 2019–20 Australian megafires, *Nat. Sustain.*, 4, 42–47, [https://doi.org/10.1038/s41893-](https://doi.org/10.1038/s41893-020-00610-5)
 912 020-00610-5, 2021.

913 Jones, M. W., Abatzoglou, J. T., Veraverbeke, S., Andela, N., Lasslop, G., Forkel, M., Smith, A.
 914 J. P., Burton, C., Betts, R. A., van der Werf, G. R., Sitch, S., Canadell, J. G., Santín, C.,
 915 Kolden, C., Doerr, S. H., and Le Quéré, C.: Global and Regional Trends and Drivers of Fire
 916 Under Climate Change, *Rev. Geophys.*, 60, e2020RG000726,
 917 <https://doi.org/10.1029/2020RG000726>, 2022.

918 Kloster, S., Dentener, F., Feichter, J., Raes, F., Lohmann, U., Roeckner, E., and Fischer-Bruns, I.:
 919 A GCM study of future climate response to aerosol pollution reductions, *Clim. Dyn.*, 34,
 920 1177–1194, <https://doi.org/10.1007/s00382-009-0573-0>, 2010.

921 Lau, K.-M. and Kim, K.-M.: Observational relationships between aerosol and Asian monsoon
 922 rainfall, and circulation, *Geophys. Res. Lett.*, 33, 2006GL027546,
 923 <https://doi.org/10.1029/2006GL027546>, 2006.

924 Leibensperger, E. M., Mickley, L. J., Jacob, D. J., Chen, W.-T., Seinfeld, J. H., Nenes, A., Adams,
 925 P. J., Streets, D. G., Kumar, N., and Rind, D.: Climatic effects of 1950–2050 changes in US
 926 anthropogenic aerosols – Part 1: Aerosol trends and radiative forcing, *Atmos. Chem. Phys.*,
 927 12, 3333–3348, <https://doi.org/10.5194/acp-12-3333-2012>, 2012.

928 Liu, C., Yang, Y., Wang, H., Ren, L., Wei, J., Wang, P., and Liao, H.: Influence of Spatial Dipole
 929 Pattern in Asian Aerosol Changes on East Asian Summer Monsoon, *J. Climate*, 36, 1575–
 930 1585, <https://doi.org/10.1175/JCLI-D-22-0335.1>, 2023.

931 Liu, X., Ma, P.-L., Wang, H., Tilmes, S., Singh, B., Easter, R. C., Ghan, S. J., and Rasch, P. J.:
 932 Description and evaluation of a new four-mode version of the Modal Aerosol Module
 933 (MAM4) within version 5.3 of the Community Atmosphere Model, *Geosci. Model Dev.*, 9,
 934 505–522, <https://doi.org/10.5194/gmd-9-505-2016>, 2016.

935 Loeb, N. G., Doelling, D. R., Wang, H., Su, W., Nguyen, C., Corbett, J. G., Liang, L., Mitrescu,
 936 C., Rose, F. G., and Kato, S.: Clouds and the Earth’s Radiant Energy System (CERES) Energy
 937 Balanced and Filled (EBAF) Top-of-Atmosphere (TOA) Edition-4.0 Data Product, *J. Climate*,
 938 31, 895–918, <https://doi.org/10.1175/JCLI-D-17-0208.1>, 2018.

939 Ming, Y. and Ramaswamy, V.: Nonlinear Climate and Hydrological Responses to Aerosol Effects,
 940 *J. Climate*, 22, 1329–1339, <https://doi.org/10.1175/2008JCLI2362.1>, 2009.

941 Moritz, M. A., Batllori, E., Bradstock, R. A., Gill, A. M., Handmer, J., Hessburg, P. F., Leonard,
 942 J., McCaffrey, S., Odion, D. C., Schoennagel, T., and Syphard, A. D.: Learning to coexist
 943 with wildfire, *Nature*, 515, 58–66, <https://doi.org/10.1038/nature13946>, 2014.

944 Nicholls, N.: Detecting and attributing Australian climate change: a review, *Aust. Meteorol. Mag.*,
945 2006.

946 Oh, H. and Ha, K.-J.: Thermodynamic characteristics and responses to ENSO of dominant
947 intraseasonal modes in the East Asian summer monsoon, *Clim. Dyn.*, 44, 1751–1766,
948 <https://doi.org/10.1007/s00382-014-2268-4>, 2015.

949 Pozzoli, L., Janssens-Maenhout, G., Diehl, T., Bey, I., Schultz, M. G., Feichter, J., Vignati, E., and
950 Dentener, F.: Re-analysis of tropospheric sulfate aerosol and ozone for the period 1980–2005
951 using the aerosol-chemistry-climate model ECHAM5-HAMMOZ, *Atmos. Chem. Phys.*, 11,
952 9563–9594, <https://doi.org/10.5194/acp-11-9563-2011>, 2011.

953 Rauniyar, S. P. and Power, S. B.: The Impact of Anthropogenic Forcing and Natural Processes on
954 Past, Present, and Future Rainfall over Victoria, Australia, *J. Climate*, 33, 8087–8106,
955 <https://doi.org/10.1175/JCLI-D-19-0759.1>, 2020.

956 Ren, L., Yang, Y., Wang, H., Wang, P., Yue, X., and Liao, H.: Widespread Wildfires Over the
957 Western United States in 2020 Linked to Emissions Reductions During COVID-19, *Geophys.*
958 *Res. Lett.*, 49, e2022GL099308, <https://doi.org/10.1029/2022GL099308>, 2022.

959 Risbey, J. S., Pook, M. J., McIntosh, P. C., Wheeler, M. C., and Hendon, H. H.: On the Remote
960 Drivers of Rainfall Variability in Australia, *Mon. Wea. Rev.*, 137, 3233–3253,
961 <https://doi.org/10.1175/2009MWR2861.1>, 2009.

962 Rotstayn, L. D., Cai, W., Dix, M. R., Farquhar, G. D., Feng, Y., Ginoux, P., Herzog, M., Ito, A.,
963 Penner, J. E., Roderick, M. L., and Wang, M.: Have Australian rainfall and cloudiness
964 increased due to the remote effects of Asian anthropogenic aerosols?, *J. Geophys. Res.:*
965 *Atmos.*, 112, 2006JD007712, <https://doi.org/10.1029/2006JD007712>, 2007.

966 Samset, B. H., Lund, M. T., Bollasina, M., Myhre, G., and Wilcox, L.: Emerging Asian aerosol
967 patterns, *Nat. Geosci.*, 12, 582–584, <https://doi.org/10.1038/s41561-019-0424-5>, 2019.

968 Schiemann, R., Lüthi, D., and Schär, C.: Seasonality and Interannual Variability of the Westerly
969 Jet in the Tibetan Plateau Region, *J. Climate*, 22, 2940–2957,
970 <https://doi.org/10.1175/2008JCLI2625.1>, 2009.

971 Seager, R., Hooks, A., Williams, A. P., Cook, B., Nakamura, J., and Henderson, N.: Climatology,
972 Variability, and Trends in the U.S. Vapor Pressure Deficit, an Important Fire-Related
973 Meteorological Quantity, *J. Appl. Meteorol. Clim.*, 54, 1121–1141,
974 <https://doi.org/10.1175/JAMC-D-14-0321.1>, 2015.

975 Seneviratne, S. I., Lüthi, D., Litschi, M., and Schär, C.: Land–atmosphere coupling and climate
976 change in Europe, *Nature*, 443, 205–209, <https://doi.org/10.1038/nature05095>, 2006.

977 Sharples, J. J., McRae, R. H. D., Weber, R. O., and Gill, A. M.: A simple index for assessing fire
978 danger rating, *Environ. Modell. Softw.*, 24, 764–774,
979 <https://doi.org/10.1016/j.envsoft.2008.11.004>, 2009.

980 Shi, G., Yan, H., Zhang, W., Dodson, J., Heijnis, H., and Burrows, M.: Rapid warming has resulted
 981 in more wildfires in northeastern Australia, *Sci. Total Environ.*, 771, 144888,
 982 <https://doi.org/10.1016/j.scitotenv.2020.144888>, 2021.

983 Skofronick-Jackson, G., Petersen, W. A., Berg, W., Kidd, C., Stocker, E. F., Kirschbaum, D. B.,
 984 Kakar, R., Braun, S. A., Huffman, G. J., Iguchi, T., Kirstetter, P. E., Kummerow, C.,
 985 Meneghini, R., Oki, R., Olson, W. S., Takayabu, Y. N., Furukawa, K., and Wilheit, T.: The
 986 Global Precipitation Measurement (GPM) Mission for Science and Society, *Bull. Am.*
 987 *Meteorol. Soc.*, 98, 1679–1695, <https://doi.org/10.1175/BAMS-D-15-00306.1>, 2017.

988 Streets, D. G., Yan, F., Chin, M., Diehl, T., Mahowald, N., Schultz, M., Wild, M., Wu, Y., and
 989 Yu, C.: Anthropogenic and natural contributions to regional trends in aerosol optical depth,
 990 1980–2006, *J. Geophys. Res.: Atmos.*, 114, 2008JD011624,
 991 <https://doi.org/10.1029/2008JD011624>, 2009.

992 Su, H., Yang, Z., Dickinson, R. E., and Wei, J.: Spring soil moisture-precipitation feedback in the
 993 Southern Great Plains: How is it related to large-scale atmospheric conditions?, *Geophys.*
 994 *Res. Lett.*, 41, 1283–1289, <https://doi.org/10.1002/2013GL058931>, 2014.

995 Turnock, S. T., Allen, R. J., Andrews, M., Bauer, S. E., Deushi, M., Emmons, L., Good, P.,
 996 Horowitz, L., John, J. G., Michou, M., Nabat, P., Naik, V., Neubauer, D., O'Connor, F. M.,
 997 Olivie, D., Oshima, N., Schulz, M., Sellar, A., Shim, S., Takemura, T., Tilmes, S., Tsigaridis,
 998 K., Wu, T., and Zhang, J.: Historical and future changes in air pollutants from CMIP6 models,
 999 *Atmos. Chem. Phys.*, 20, 14547–14579, <https://doi.org/10.5194/acp-20-14547-2020>, 2020.

1000 Undorf, S., Polson, D., Bollasina, M. A., Ming, Y., Schurer, A., and Hegerl, G. C.: Detectable
 1001 Impact of Local and Remote Anthropogenic Aerosols on the 20th Century Changes of West
 1002 African and South Asian Monsoon Precipitation, *J. Geophys. Res.: Atmos.*, 123, 4871–4889,
 1003 <https://doi.org/10.1029/2017JD027711>, 2018.

1004 Van Marle, M. J. E., Kloster, S., Magi, B. I., Marlon, J. R., Daniau, A.-L., Field, R. D., Arneeth,
 1005 A., Forrest, M., Hantson, S., Kehrwald, N. M., Knorr, W., Lasslop, G., Li, F., Mangeon, S.,
 1006 Yue, C., Kaiser, J. W., and Van Der Werf, G. R.: Historic global biomass burning emissions
 1007 for CMIP6 (BB4CMIP) based on merging satellite observations with proxies and fire models
 1008 (1750–2015), *Geosci. Model Dev.*, 10, 3329–3357, [https://doi.org/10.5194/gmd-10-3329-](https://doi.org/10.5194/gmd-10-3329-2017)
 1009 2017, 2017.

1010 Wang, B., Biasutti, M., Byrne, M. P., Castro, C., Chang, C.-P., Cook, K., Fu, R., Grimm, A. M.,
 1011 Ha, K.-J., Hendon, H., Kitoh, A., Krishnan, R., Lee, J.-Y., Li, J., Liu, J., Moise, A., Pascale,
 1012 S., Roxy, M. K., Seth, A., Sui, C.-H., Turner, A., Yang, S., Yun, K.-S., Zhang, L., and Zhou,
 1013 T.: Monsoons Climate Change Assessment, *Bull. Am. Meteorol. Soc.*, 102, E1–E19,
 1014 <https://doi.org/10.1175/BAMS-D-19-0335.1>, 2021.

1015 Wang, H., Easter, R. C., Rasch, P. J., Wang, M., Liu, X., Ghan, S. J., Qian, Y., Yoon, J.-H., Ma,
 1016 P.-L., and Vinoj, V.: Sensitivity of remote aerosol distributions to representation of cloud–
 1017 aerosol interactions in a global climate model, *Geosci. Model Dev.*, 6, 765–782,
 1018 <https://doi.org/10.5194/gmd-6-765-2013>, 2013.

- 1019 Wang, P., Yang, Y., Xue, D., Ren, L., Tang, J., Leung, L. R., and Liao, H.: Aerosols overtake
1020 greenhouse gases causing a warmer climate and more weather extremes toward carbon
1021 neutrality, *Nat. Commun.*, 14, 7257, <https://doi.org/10.1038/s41467-023-42891-2>, 2023.
- 1022 Wang, Z., Zhang, H., and Zhang, X.: Projected response of East Asian summer monsoon system
1023 to future reductions in emissions of anthropogenic aerosols and their precursors, *Clim. Dyn.*,
1024 47, 1455–1468, <https://doi.org/10.1007/s00382-015-2912-7>, 2016.
- 1025 Wang, Z., Lin, L., Xu, Y., Che, H., Zhang, X., Zhang, H., Dong, W., Wang, C., Gui, K., and Xie,
1026 B.: Incorrect Asian aerosols affecting the attribution and projection of regional climate change
1027 in CMIP6 models, *npj Clim. Atmos. Sci.*, 4, 2, <https://doi.org/10.1038/s41612-020-00159-2>,
1028 2021.
- 1029 Ward, M., Tulloch, A. I. T., Radford, J. Q., Williams, B. A., Reside, A. E., Macdonald, S. L.,
1030 Mayfield, H. J., Maron, M., Possingham, H. P., Vine, S. J., O'Connor, J. L., Massingham, E.
1031 J., Greenville, A. C., Woinarski, J. C. Z., Garnett, S. T., Lintermans, M., Scheele, B. C.,
1032 Carwardine, J., Nimmo, D. G., Lindenmayer, D. B., Kooyman, R. M., Simmonds, J. S., Sonter,
1033 L. J., and Watson, J. E. M.: Impact of 2019–2020 mega-fires on Australian fauna habitat, *Nat.*
1034 *Ecol. Evol.*, 4, 1321–1326, <https://doi.org/10.1038/s41559-020-1251-1>, 2020.
- 1035 Wasko, C., Shao, Y., Vogel, E., Wilson, L., Wang, Q. J., Frost, A., and Donnelly, C.:
1036 Understanding trends in hydrologic extremes across Australia, *J. Hydrol.*, 593, 125877,
1037 <https://doi.org/10.1016/j.jhydrol.2020.125877>, 2021.
- 1038 Yang, Y., Zeng, L., Wang, H., Wang, P., and Liao, H.: Climate effects of future aerosol reductions
1039 for achieving carbon neutrality in China, *Sci. Bull.*, 68, 902–905,
1040 <https://doi.org/10.1016/j.scib.2023.03.048>, 2023.
- 1041 Zacharakis, I. and Tsihrintzis, V. A.: Integrated wildfire danger models and factors: A review, *Sci.*
1042 *Total Environ.*, 899, 165704, <https://doi.org/10.1016/j.scitotenv.2023.165704>, 2023.
- 1043 Zeng, L., Yang, Y., Wang, H., Wang, J., Li, J., Ren, L., Li, H., Zhou, Y., Wang, P., and Liao, H.:
1044 Intensified modulation of winter aerosol pollution in China by El Niño with short duration,
1045 *Atmos. Chem. Phys.*, 21, 10745–10761, <https://doi.org/10.5194/acp-21-10745-2021>, 2021.
- 1046 Zhang, Q., Zheng, Y., Tong, D., Shao, M., Wang, S., Zhang, Y., Xu, X., Wang, J., He, H., Liu,
1047 W., Ding, Y., Lei, Y., Li, J., Wang, Z., Zhang, X., Wang, Y., Cheng, J., Liu, Y., Shi, Q., Yan,
1048 L., Geng, G., Hong, C., Li, M., Liu, F., Zheng, B., Cao, J., Ding, A., Gao, J., Fu, Q., Huo, J.,
1049 Liu, B., Liu, Z., Yang, F., He, K., and Hao, J.: Drivers of improved PM_{2.5} air quality in China
1050 from 2013 to 2017, *Proc. Natl. Acad. Sci.*, 116, 24463–24469,
1051 <https://doi.org/10.1073/pnas.1907956116>, 2019.
- 1052 Zheng, B., Tong, D., Li, M., Liu, F., Hong, C., Geng, G., Li, H., Li, X., Peng, L., Qi, J., Yan, L.,
1053 Zhang, Y., Zhao, H., Zheng, Y., He, K., and Zhang, Q.: Trends in China's anthropogenic
1054 emissions since 2010 as the consequence of clean air actions, *Atmos. Chem. Phys.*, 18,
1055 14095–14111, <https://doi.org/10.5194/acp-18-14095-2018>, 2018.

1056 Zheng, Y., Xue, T., Zhang, Q., Geng, G., Tong, D., Li, X., and He, K.: Air quality improvements
1057 and health benefits from China's clean air action since 2013, *Environ. Res. Lett.*, 12, 114020,
1058 <https://doi.org/10.1088/1748-9326/aa8a32>, 2017.

1059 Zheng, Y., Zhang, Q., Tong, D., Davis, S. J., and Caldeira, K.: Climate effects of China's efforts
1060 to improve its air quality, *Environ. Res. Lett.*, 15, 104052, [https://doi.org/10.1088/1748-](https://doi.org/10.1088/1748-9326/ab9e21)
1061 [9326/ab9e21](https://doi.org/10.1088/1748-9326/ab9e21), 2020.

1062

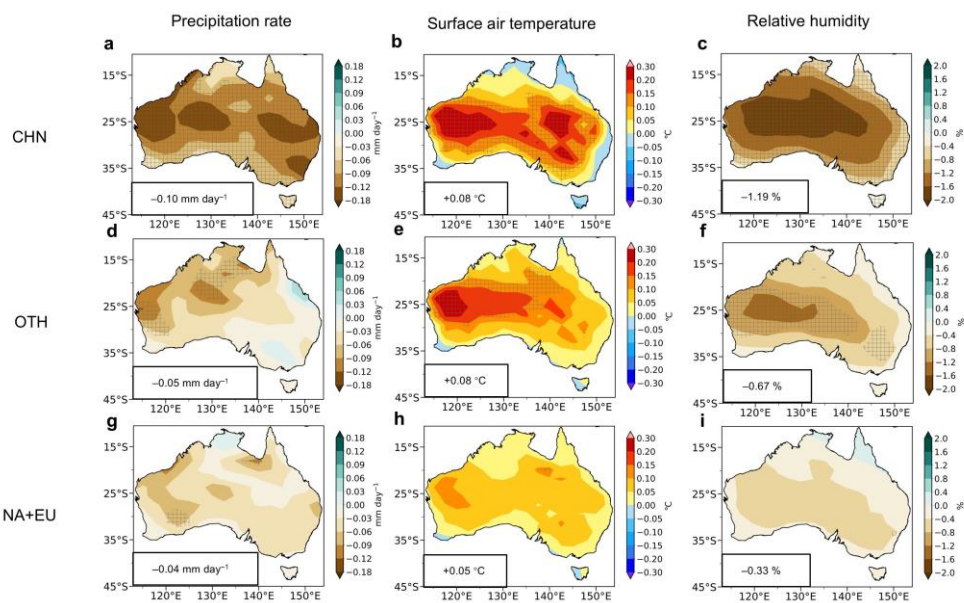
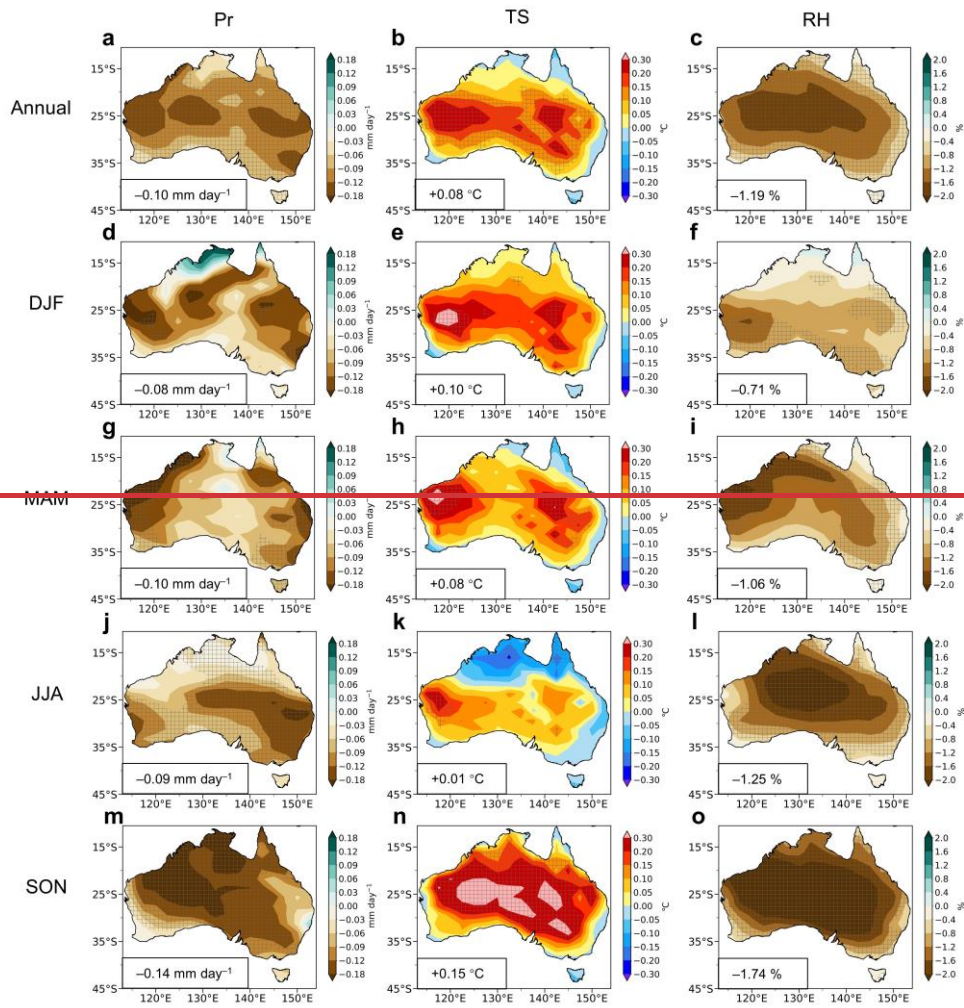


Figure 1. Simulated changes in precipitation rate, surface air temperature and relative humidity in Australia due to aerosol changes in China between 2013 and 2019. Spatial distributions of simulated differences in annual (**a–c**), DJF (**d–f**, December, January and February), MAM (**g–i**, March, April and May), JJA (**j–l**, June, July and August) and SON (**m–o**, September, October and November) mean precipitation rate (Pr, **a**, **d**, **g**, **j** and **m**, unit: mm day⁻¹), surface air temperature (TS, **b**, **e**, **h**, **k** and **n**, unit: °C) and relative humidity (RH, **c**, **f**, **i**, **l** and **o**, unit: %) in Australia between BASE and CHN (CHN minus BASE, **a–c**), between BASE and OTH (OTH minus BASE, **d–f**), and between BASE and NAEU (NAEU minus BASE, **g–i**). The shaded areas indicate results are statistically significant at the 90% confidence level. Regional averages over Australia are noted at the bottom-left corner of each panel.

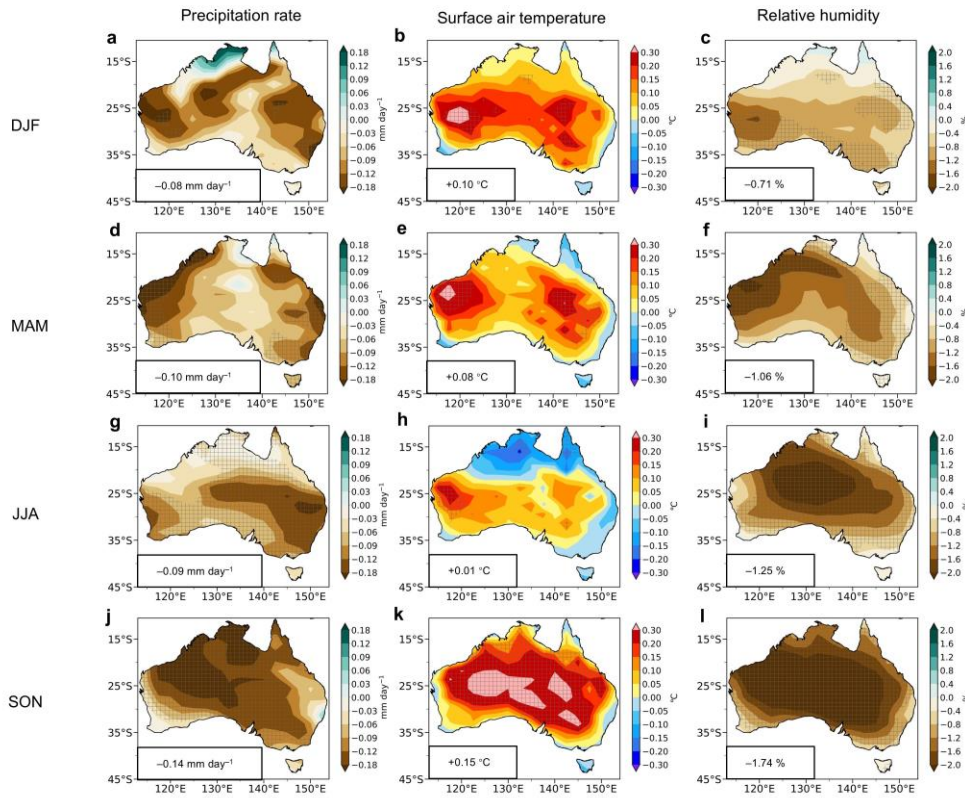


Figure 2. Simulated changes in precipitation rate, surface air temperature and relative humidity in Australia due to aerosol changes in China between 2013 and 2019. Spatial distributions of simulated differences in DJF (December, January and February, **a–c**), MAM (March, April and May, **d–f**), JJA (June, July and August, **g–i**) and SON (September, October

and November, **j–l**) mean precipitation rate (Pr, **a, d, g, and j**, unit: mm day⁻¹), surface air temperature (TS, **b, e, h, and k**, unit: °C) and relative humidity (RH, **c, f, i, and l**, unit: %) in Australia between BASE and CHN (CHN minus BASE). The shaded areas indicate results are statistically significant at the 90% confidence level. Regional averages over Australia are noted at the bottom-left corner of each panel.

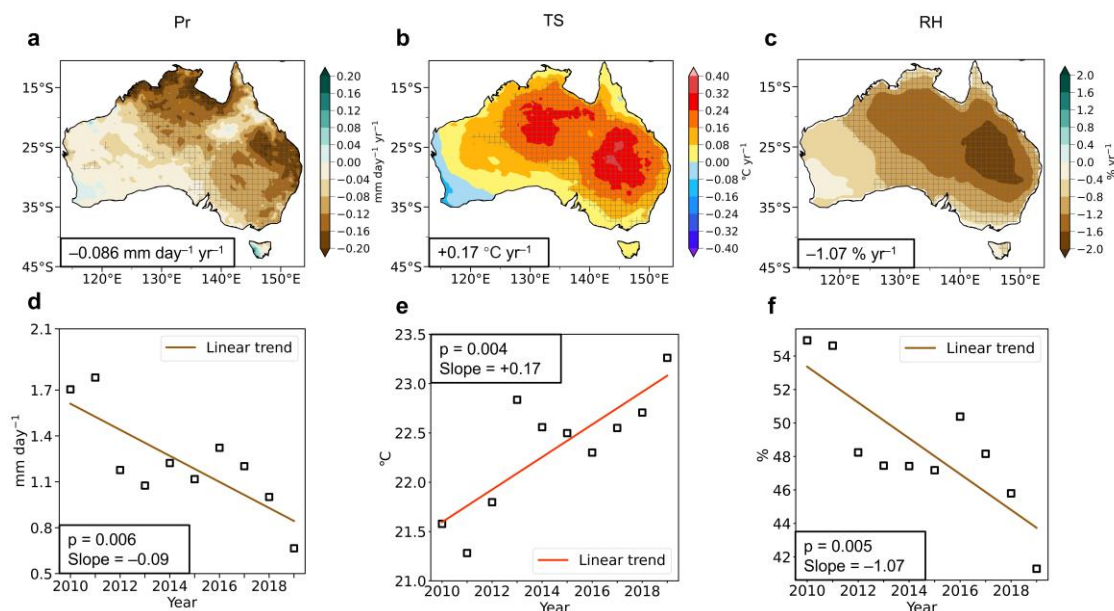


Figure 23. Linear trends of observed precipitation rate, surface air temperature and relative humidity in Australia based on ERA5. Spatial distributions of linear trends (a, b, and c) and time series (d, e, and f) of annual mean precipitation rate (Pr, a and d, unit: mm day^{-1}), surface air temperature (TS, b and e, unit: $^{\circ}\text{C}$) and relative humidity (RH, c and f, unit: $\%$) in Australia during 2010–2019 from ERA5 reanalysis. The shaded areas indicate trends are statistically significant at the 90% confidence level. Regional averages over Australia are noted at the bottom-left corner of panels a, b, and c. The p values and slopes of linear trends are noted in panels d, e, and f.

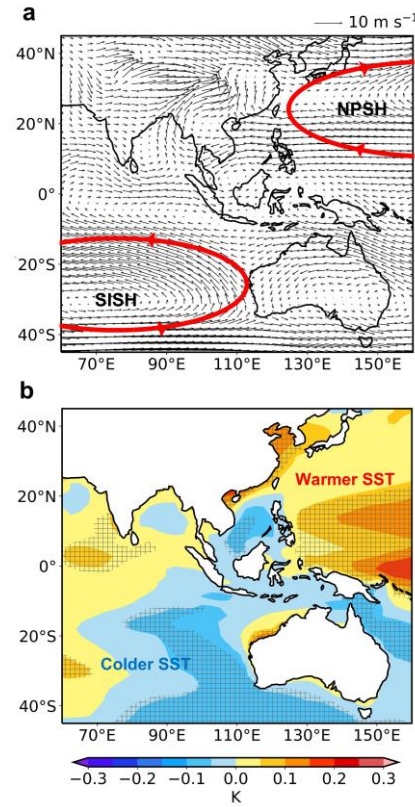


Figure 4. Climatological mean wind fields at 850 hPa and Simulated sea surface temperature changes due to aerosol changes in China between 2013 and 2019. a, Climatological mean wind fields (unit: m s⁻¹, vectors) at 850 hPa from the BASE experiment. NPSH and SISH shown in red circles represents North Pacific Subtropical High and Southern Indian ocean Subtropical High, respectively. **b,** Spatial distributions of simulated differences in annual mean sea surface temperature (SST, unit: mm day⁻¹) in Australia between BASE and CHN (CHN minus BASE). The shaded areas indicate results are statistically significant at the 90% confidence level.

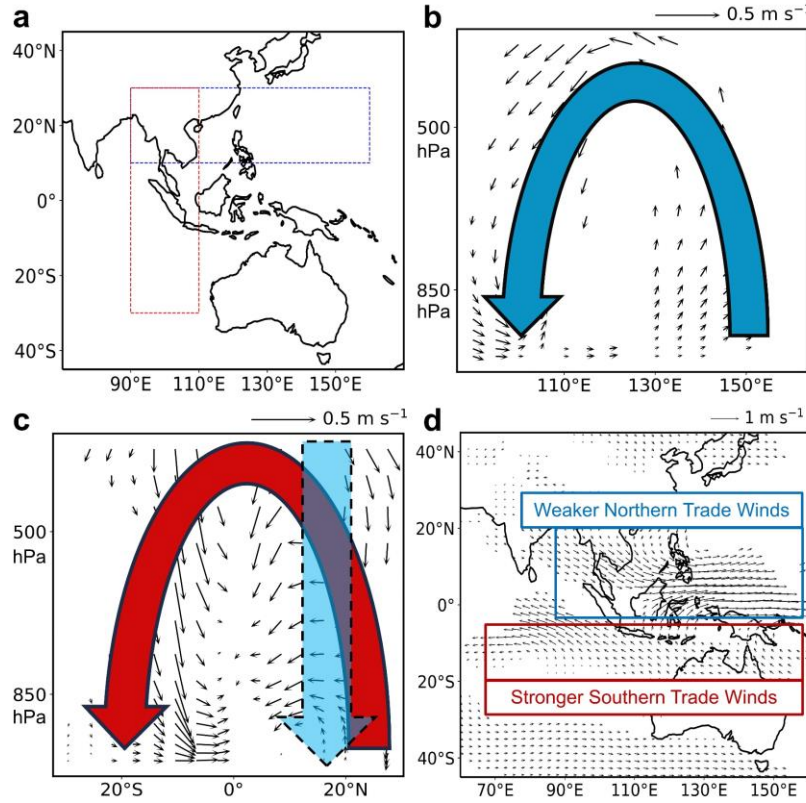


Figure 35. Simulated changes in vertical circulations and 850 hPa wind fields in Asia-Pacific regions due to aerosol changes in China between 2013 and 2019. Panel b and c shows pressure–longitude and pressure–latitude cross-section of responses in annual mean atmospheric circulations (unit: m s^{-1} , vectors), respectively, over the areas marked with the blue and red box in panel a. Panel d shows annual mean changes in wind fields (unit: m s^{-1} , vectors) at 850 hPa in Asia-Pacific regions. Only atmospheric circulations and winds statistically significant at the 90% confidence level are shown.

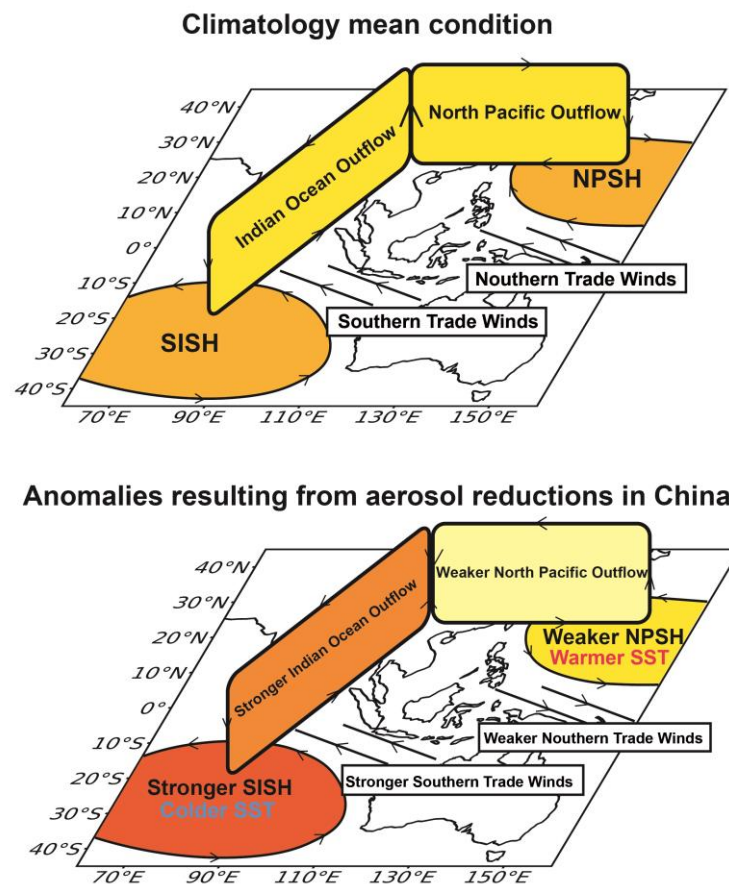
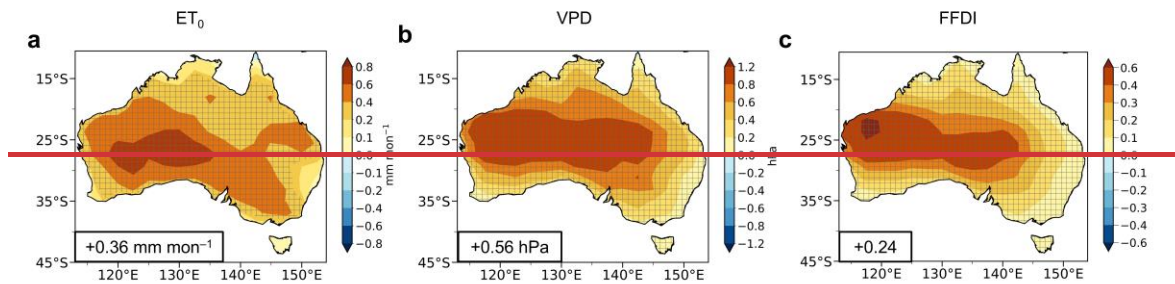


Figure 4.

Figure 6. Schematic of the response in large-scale 3D circulations in the Asian-Pacific region to aerosol reductions in China. The top panel shows climatology mean condition, and the bottom panel shows anomalies resulting from aerosol reductions in China.

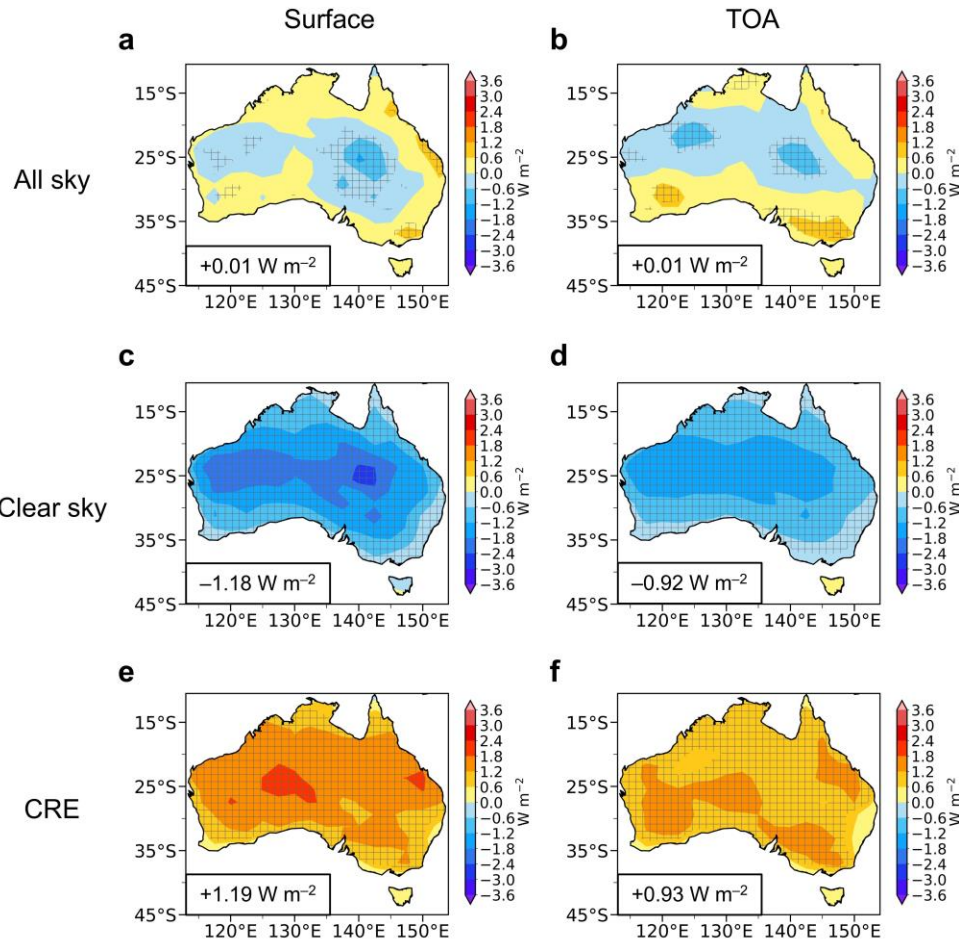


Figure 7. Simulated changes in surface and Top of the Atmosphere (TOA) net total radiative flux under all sky conditions, under clear sky conditions, and from cloud radiative effects in Australia due to aerosol changes in China between 2013 and 2019. Spatial distributions of simulated differences in annual mean surface (a, c, and e) and Top of the Atmosphere (TOA, b, d, and f) net total radiative flux (unit: W m^{-2}) under all sky conditions (a and b), under clear sky conditions (c and d), and from cloud radiative effects (CRE, e and f) in Australia between BASE and CHN (CHN minus BASE). Cloud radiative effects refer to differences under all sky and clear sky conditions (All sky minus Clear sky). The shaded areas indicate results are statistically significant at the 90% confidence level. Regional averages of the responses over Australia are noted at the bottom-left corner of each panel.

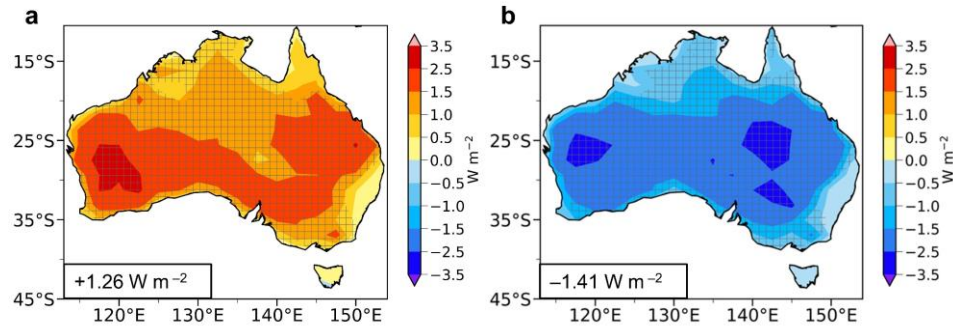


Figure 8. Simulated changes in surface upward sensible and latent heat flux in Australia due to aerosol changes in China between 2013 and 2019. Spatial distributions of simulated differences in annual mean surface upward sensible (a) and latent (b) heat flux (unit: W m^{-2}) in Australia between BASE and CHN (CHN minus BASE). The shaded areas indicate results are statistically significant at the 90% confidence level. Regional averages over Australia are noted at the bottom-left corner of each panel.

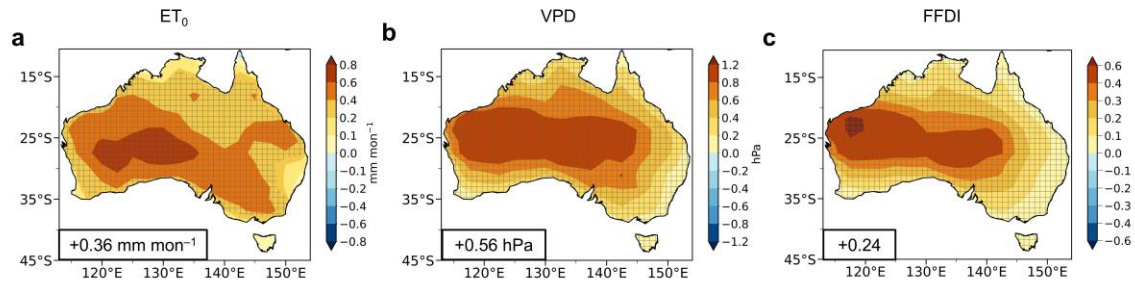


Figure 9. Simulated changes in reference potential evapotranspiration, vapor pressure deficit, and McArthur forest fire danger index during fire seasons in Australia due to aerosol changes in China between 2013 and 2019. Spatial distributions of simulated changes in reference potential evapotranspiration (ET_0 , **a**, unit: mm mon^{-1}), vapor pressure deficit (VPD, **b**, unit: hPa), and McArthur forest fire danger index (FFDI, **c**, unitless) during fire seasons (austral spring and summer, from September to the February of the next year) in Australia between BASE and CHN (CHN minus BASE). The shaded areas indicate results are statistically significant at the 90% confidence level. Regional averages over Australia are noted at the bottom-left corner of each panel.